Channeling of Radiations:

from Crystal Undulators to Capillary Waveguides

Sultan B. Dabagov

INFN - Laboratori Nazionali di Frascati, Frascati

RAS - P.N. Lebedev Physical Institute, Moscow

@ Channeling: Orientational Effects of Transmission

- 1962-63:
  - Robinson & Oen:
  - Piercy & Lutz:
- 1965:
  - Lindhard:
  - …..
  - Andersen
  - Uggerhoj
  - Kagan
  - Kononez
  - Firsov
  - Tsyganov
  - Gibson
  - Kumakhov
  - Beloshitsky
  - Gemmel
  - Appleton
  - …..

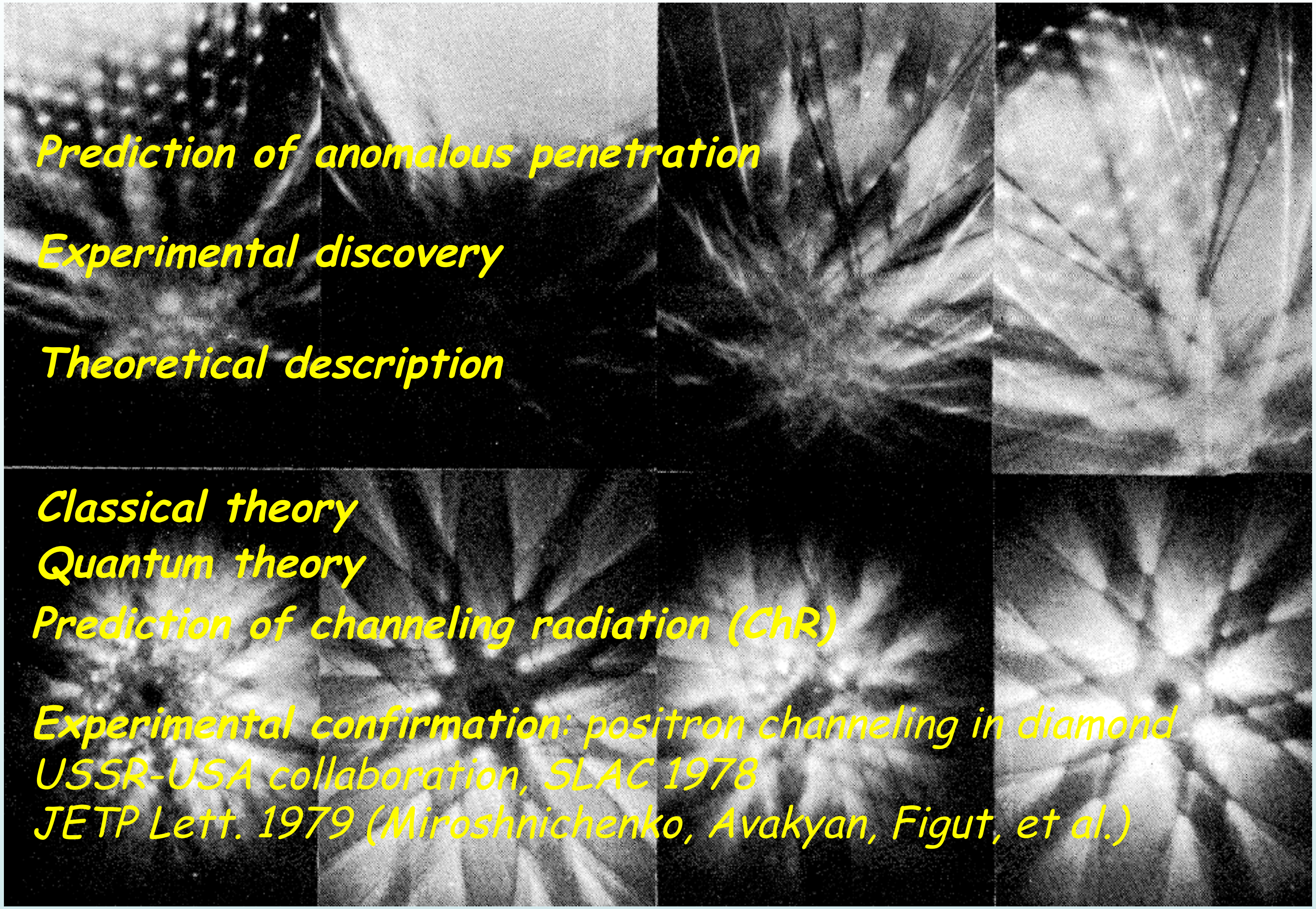

Rev. Mod. Phys. 1974: 1 MeV e^- @ Cu crystal

more than 1000 articles + a number of monographs

@ Channeling of Charged Particles

@ Amorphous:

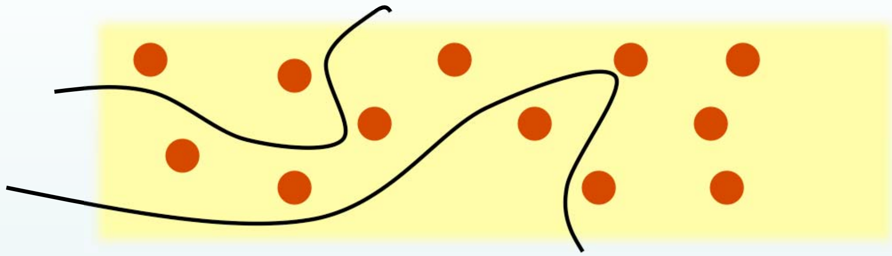

@ Channeling:

planar channeling

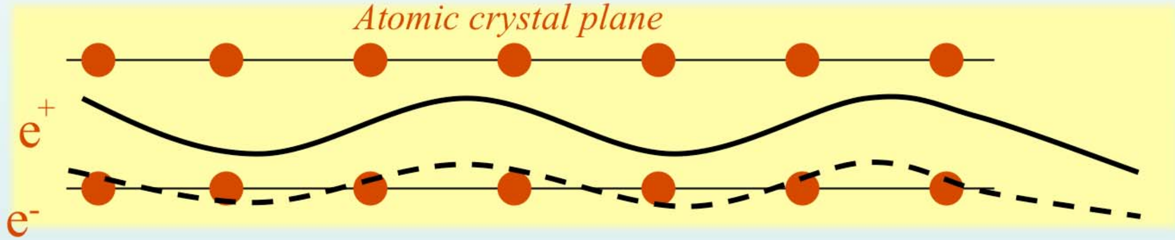

axial channeling

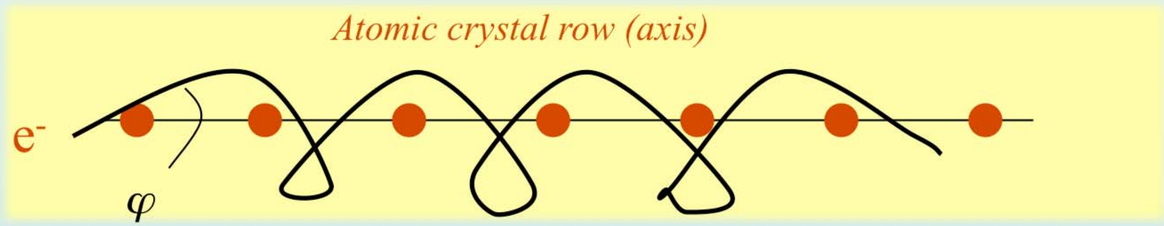

$\varphi << 1 \qquad (\varphi < \varphi_L \sim \sqrt{U/E})$ - *the Lindhard angle is the critical angle for the channeling*

@ Channeling of Charged Particles & Channeling Radiation

@ Channeling:

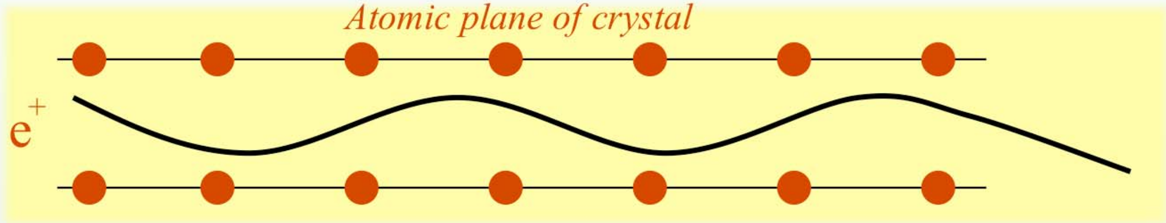

$\varphi << 1 \quad (\varphi < \varphi_L \sim \sqrt{U/E})$ - *the Lindhard angle is the critical angle for the channeling*

@ Channeling Radiation:

$$\omega = \omega(\theta) = \frac{\omega_{fi}}{1 - \beta_{\|}\cos\theta}$$

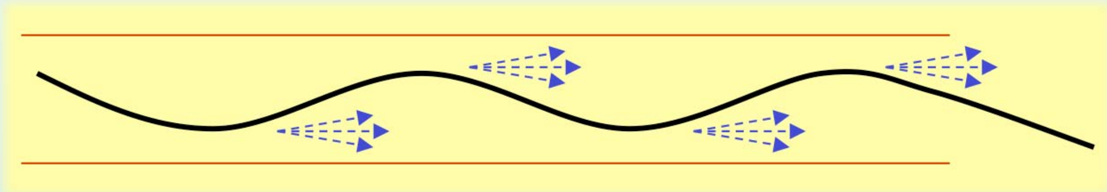

ω_{fi} - *optical frequency* ⟶ *Doppler effect* ⟶ $\omega_0\gamma^{3/2}$ - $\omega_0\gamma^{2}$

$(\gamma >> 1)$

Powerful radiation source of X-rays and γ-rays:

- polarized
- Tunable (keV - MeV)
- narrow forwarded

@ Channeling: Continuum model

$$V(r) = \frac{Z_1 Z_2 e^2}{r}\varphi(r/a)$$

screening function of Thomas-Fermi type

$$a = .8853 a_0 \left(Z_1^{1/2} + Z_2^{1/2}\right)^{-2/3}$$

screening length

$\varphi(r/a)$: $\sum_{i=1}^{3} \alpha_i \exp(-\beta_i r/a)$ Molier's potential

$1 - \left[1 + \frac{Ca}{r^2}\right]^{-1/2}$ $C^2 \approx 3$ Lindhard potential

…… Firsov, Doyle-Turner, etc.

Lindhard:

Continuum model –

continuum atomic plane/axis potential

$$V_{RS}(\rho) = \frac{1}{d}\int_{-\infty}^{+\infty} V\left(\sqrt{\rho^2 + x^2}\right)dx$$

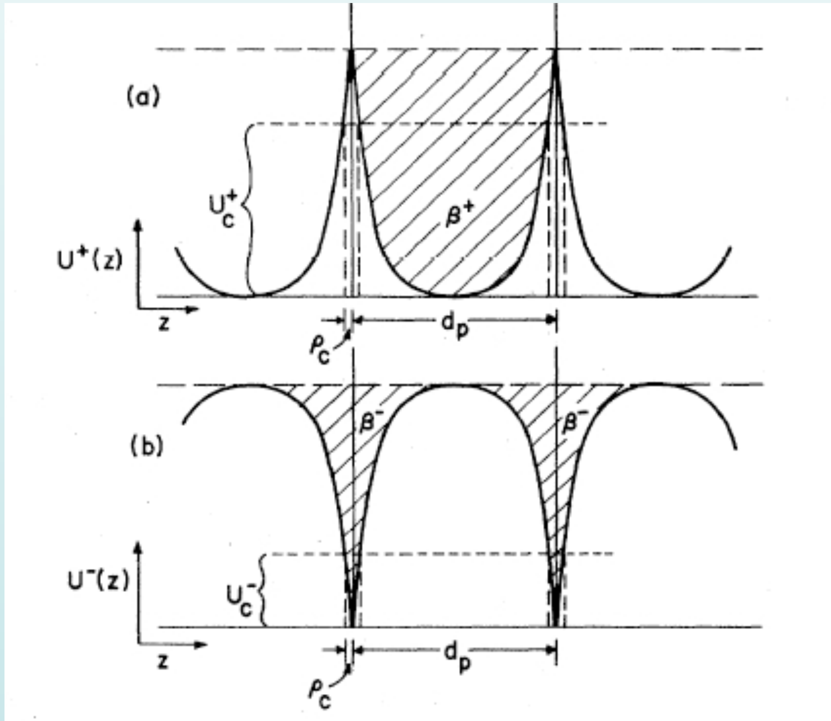

@ Channeling Radiation

@ Channeling Radiation:

$\Delta\vartheta \simeq \gamma^{-1}$

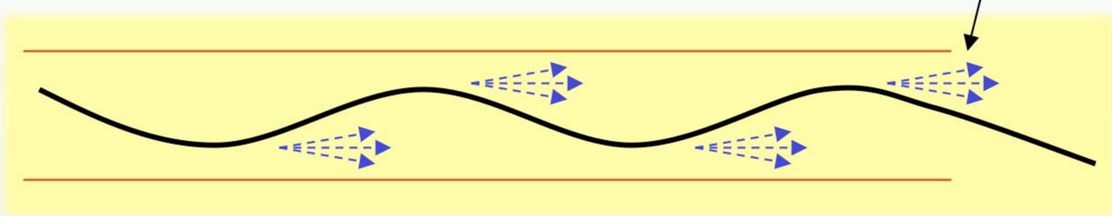

$$\omega = \omega(\theta) = \frac{\omega_{fi}}{1 - \beta_{\parallel} \cos\theta}$$

ω_{fi} *- optical frequency* ⟶ *Doppler effect* ⟶ $\omega_0\gamma^{3/2}$ - $\omega_0\gamma^2$

$(\gamma >> 1)$

Powerful radiation source of X-rays and γ-rays:

- polarized
- tunable
- narrow forwarded

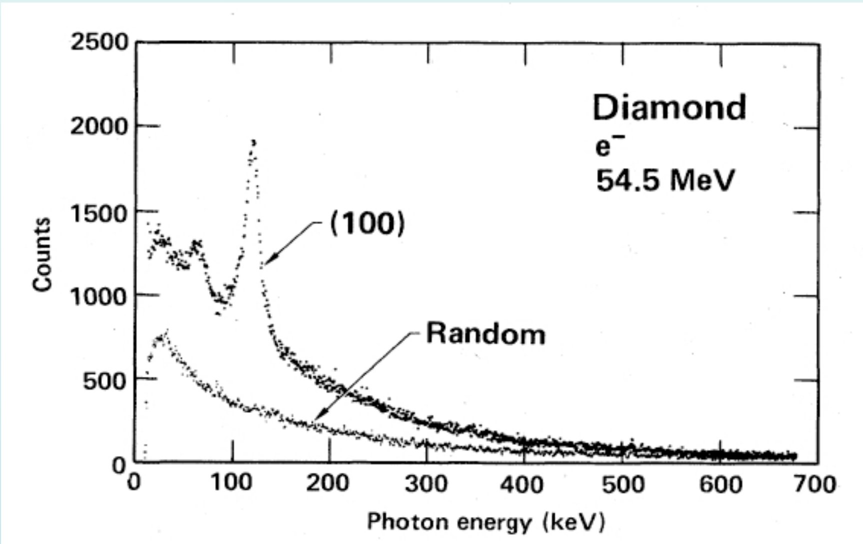

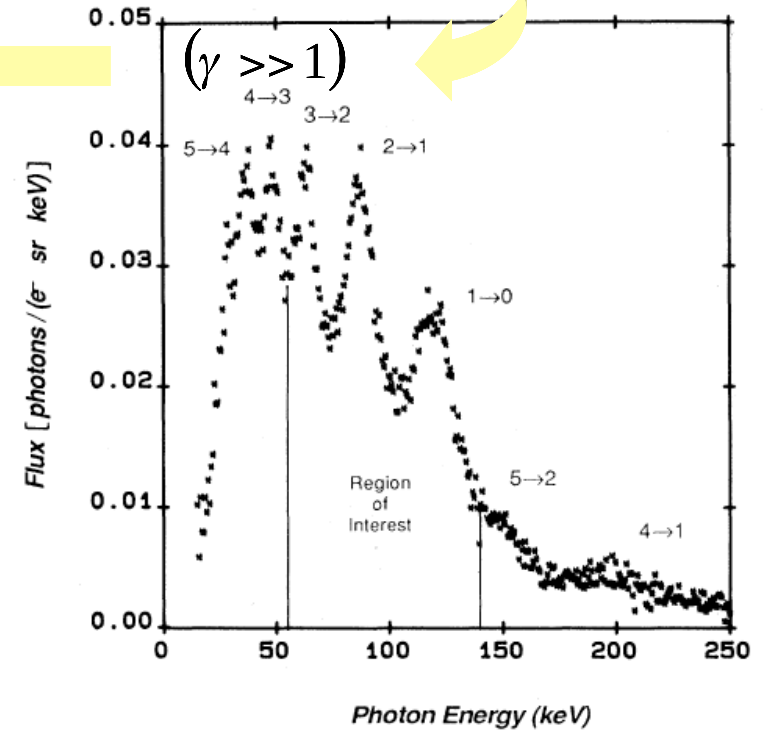

@ Bremsstrahlung & Coherent Bremsstrahlung vs Channeling Radiation

@ amorphous - electron:

- Radiation as sum of independent impacts with atoms
- Effective radius of interaction – a_{TF}
- Coherent radiation length $l_{coh} >> a_{TF}$
- Deviations in trajectory less than effective radiation angles:

$$\Delta\theta \propto a_{TF} / p \qquad \Delta\vartheta \simeq \gamma^{-1}$$

$$\left(\frac{d^2 I}{d\omega\Omega}\right)_{BR} \simeq (\pi L_R)^{-1}\gamma^2 \frac{1+\gamma^4\theta^4}{(1+\gamma^2\theta^2)^4} \longrightarrow \left(\frac{dI}{d\omega}\right)_{BR} \simeq \frac{4}{3} L_R^{-1}$$

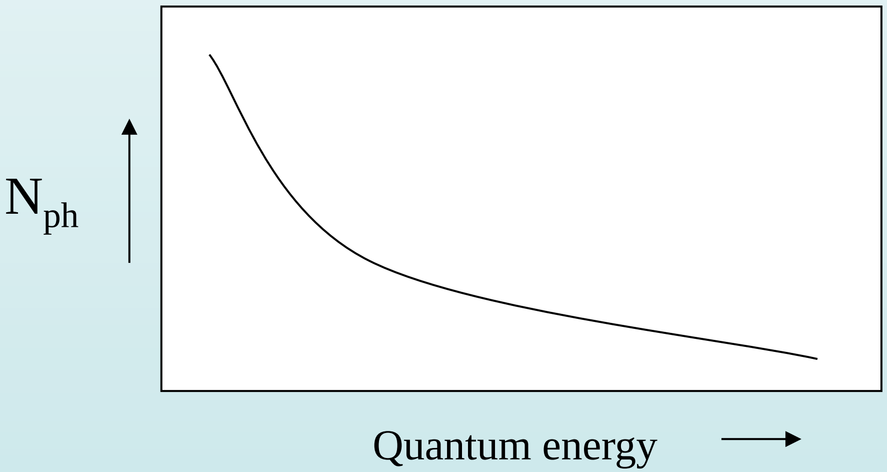

@ Bremsstrahlung & Coherent Bremsstrahlung vs Channeling Radiation

@ interference of consequent radiation events:

phase of radiation wave $\longrightarrow$ $(\omega t - \mathbf{kr}(t))$

Radiation field as interference of radiated waves:

$$l_{coh} \approx \frac{v}{\omega - \mathbf{k}\dot{\mathbf{r}}} = \frac{\lambda\beta}{1-\beta cos\theta} \longrightarrow l_{coh} \propto \gamma^2\lambda$$

Coherent radiation length can be rather large even for short wavelength

@ crystal: $l_1 = n l_{coh}$ $\quad l = d/\sin\alpha$ $\quad l_1 = \dfrac{n\lambda\beta}{1-\beta\cos\theta}$ $\quad \omega_0 \equiv \beta/l_1$

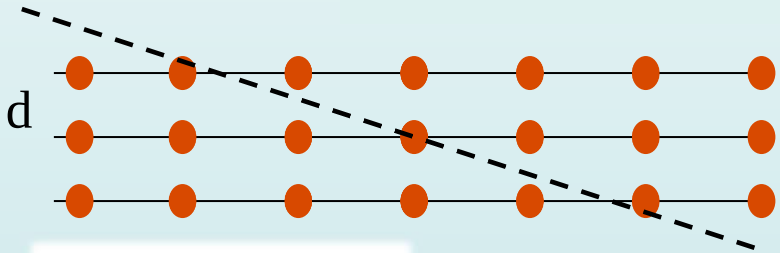

$$\omega = \frac{n\omega_0}{1-\beta\cos\theta}$$

$$\left(\frac{d^2 I}{d\omega\Omega}\right)_{CBR} \propto \delta\left(\omega(1-\beta\cos\theta) - n\omega_0\right)$$

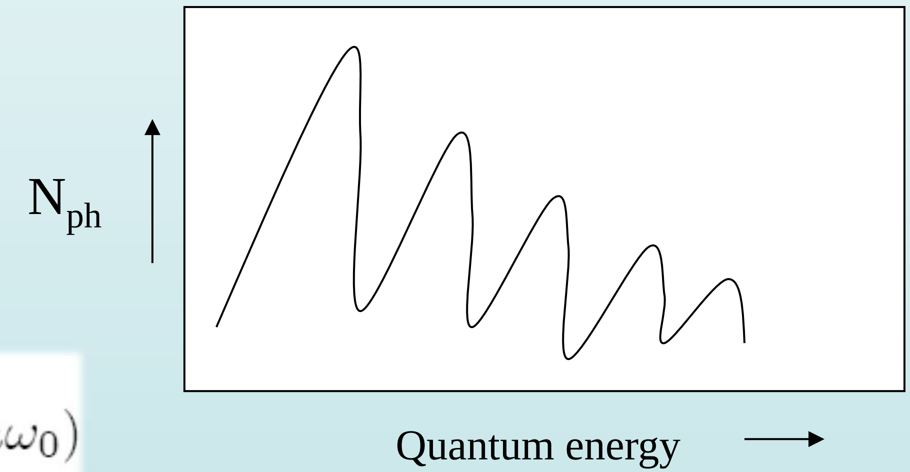

@ Bremsstrahlung & Coherent Bremsstrahlung vs Channeling Radiation

@ crystal: $\alpha \to 0$

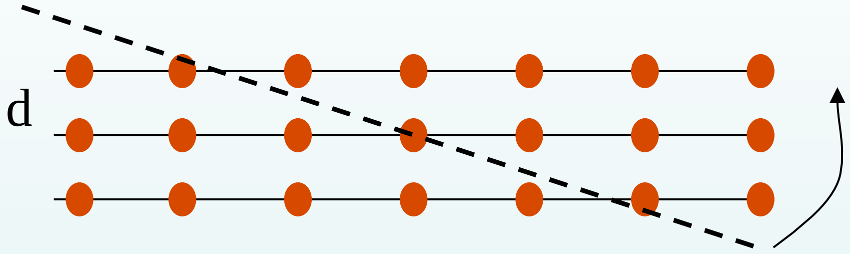

$\longrightarrow$ channeling

$$\omega = \frac{\omega_{fi}}{1 - \beta_{||}\cos\theta}$$

$$\left(\frac{dI}{d\omega}\right)_{CR} \propto \omega \left[1 - 2\left(\frac{\omega}{\omega_m}\right) + 2\left(\frac{\omega}{\omega_m}\right)^2\right], \quad \omega \le \omega_m \simeq 2\gamma^2\omega_{fi}$$

$$\frac{ChR}{B} \propto \gamma^{1/2} Z^{-2/3}$$

at definite conditions channeling radiation can be significantly powerful than bremsstrahlung

B:	CB:	ChR:
	NZe	$N \leftrightarrow \quad l_{coh} \propto \gamma^2/\omega \quad N_{eff}$
$\propto NZ^2$	$\propto (NZ)^2$	$\propto (N_{eff}Z)^2$

@ Channeling Radiation & Thomson Scattering

$$\omega_{lab}^{ChR} \approx \frac{2\gamma^2}{1+\theta^2\gamma^2}\,\omega_0^{ChR} \qquad \propto \gamma^{3/2}$$

- radiation frequency -

$$\omega_{lab}^{TS}\left\{\begin{array}{c}\vartheta = 0\\ \vartheta = \pi/2\\ \vartheta = \pi\end{array}\right\} \simeq \left\{\begin{array}{c}1\\2\\4\end{array}\right\}\frac{\gamma^2}{1+\vartheta^2\gamma^2}\omega_0^{TS} \qquad \propto \gamma^2$$

$$\left(\frac{dN_{ph}}{dt}\right)_{ChR} \propto \gamma^{1/2}$$

- number of photons per unit of time -

$$\left(\frac{dN_{ph}}{dt}\right)_{TS} \propto Const$$

$$P \propto \gamma^2$$

- radiation power -

$$P \propto \gamma^2$$

@ comparison factor:

$$f \simeq \frac{\mathbf{A}_{Ch}^2}{\mathbf{A}_{TS}^2}\frac{L_{Ch}}{L_{TS}}$$

$$L_{Ch}(z) \simeq \int_0^z N_{ch}(z)\,dz$$

→ Laser beam size & mutual orientation

@ strength parameters – crystal & field:

	Si ⟨110⟩	C ⟨100⟩	W ⟨111⟩
$\mathbf{A}_{Ch}^2$, eV/Å^3	~ 520	~ 580	~ 10000

$\mathbf{A}_{TS}^2$ ~ 700 eV/Å^3 for the 10 TW laser with a beam diameter of 0.1 mm

@ Channeling Radiation & Thomson Scattering

For X-ray frequencies: **100 MeV** electrons **channeled** in 105 μm Si (110) emit ~ 10^{-3} ph/e^-

corresponding to a Photon Flux ~ 10^8 ph/sec

ChR – effective source of photons in very wide frequency range:

- in x-ray range – higher than B, CB, and TS
- however, TS provides a higher degree of monochromatization and TS is not undergone incoherent background, which always takes place at ChR

@ Bent Crystal as Microundulator & Lasing Effect

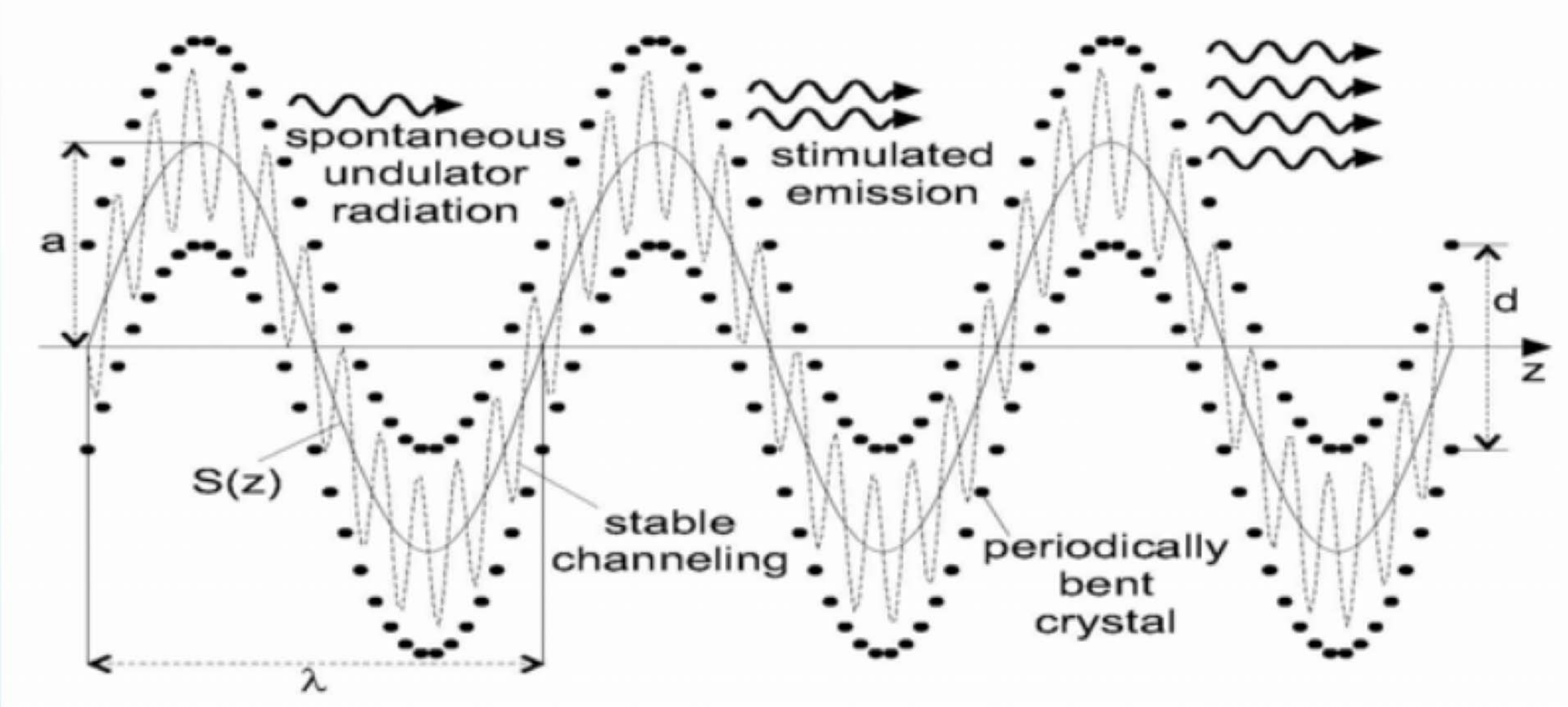

The important and novel idea consists in **realizing a microundulator**, that is a suitable periodically bent crystal, that allows to achieve much higher energy range for the emitted photons respect to the conventional free electron laser (up to 100 keV). A crystalline undulator can be realized either dynamically, using high amplitude transverse acoustic wave, or statically using graded composition of strained layers. Both methods are easily applicable by means of modern technology.

The theoretical results establish the feasibility of a crystalline undulator, but in order to make the project to advance it is mandatory to carry out experiments to test the idea and to characterize the emitted radiation as a function of several parameters.

@ BTF Layout

• BTF as unique European facility to deliver positron beams in the range of the energy required for CUP

• strong photon peak with energy from 20 keV up to 1,5 MeV should appear according well accepted channeling and undulator theories for 400-600 MeV positrons

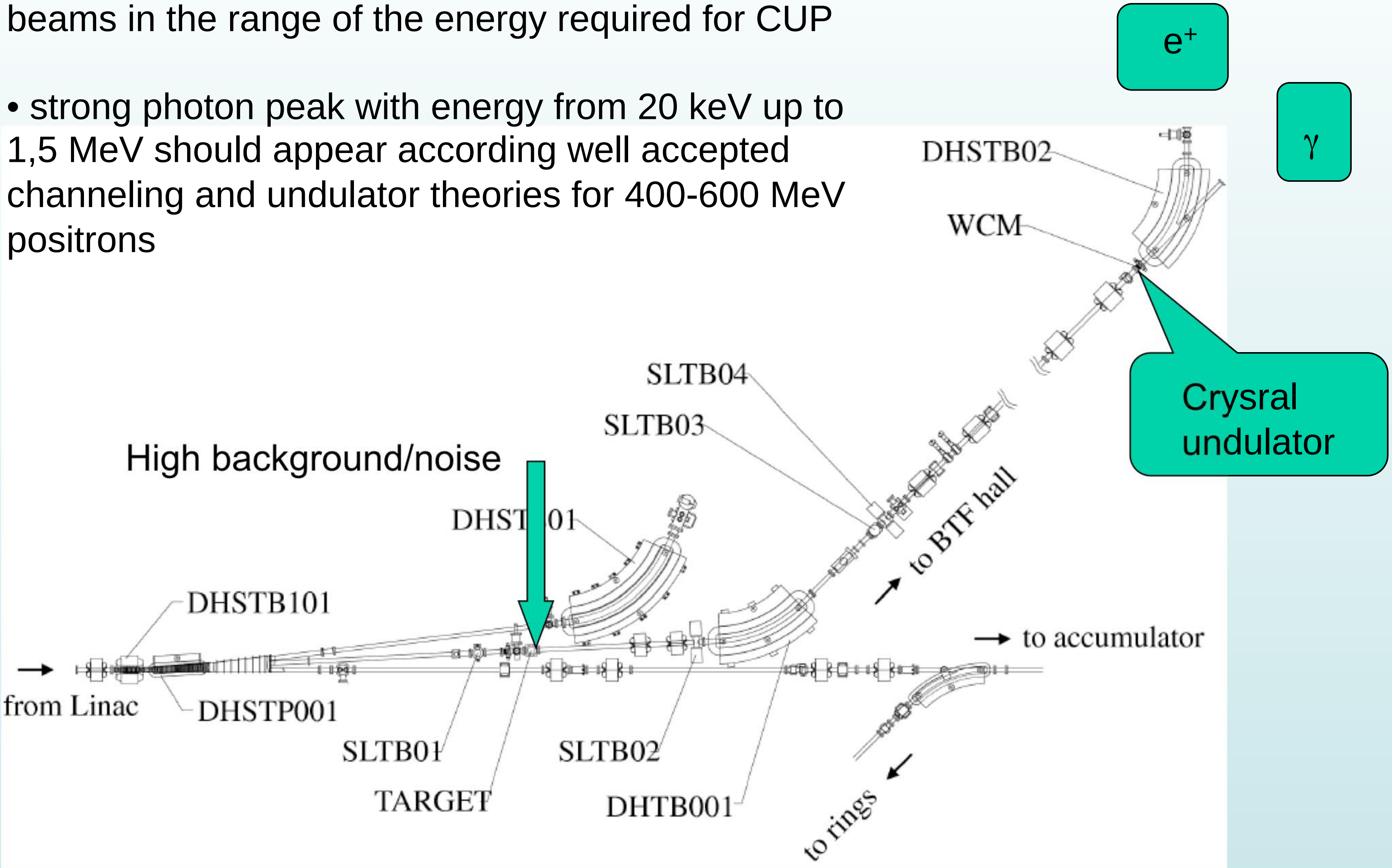

@ Crystal collimation

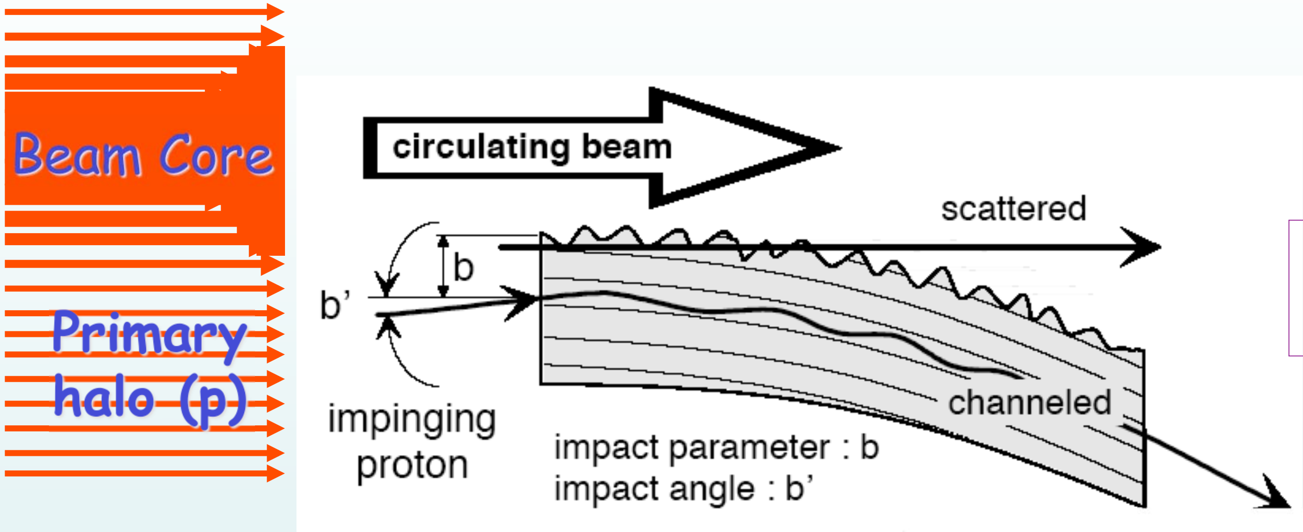

E. Tsyganov – 1975
E. Tsyganov & R.A. Carrigan - 1976
E. Tsyganov & A. Taratin - 1991

Possible processes:

- multiple scattering
- channeling
- volume capture
- de-channeling
- *volume reflection*

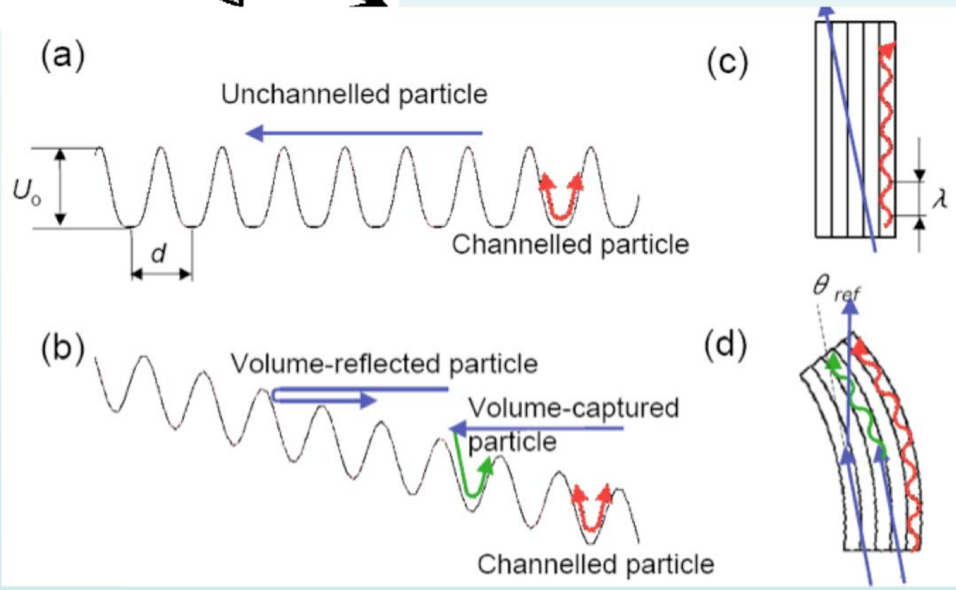

- **Primary halo directly extracted!**
- **Much less secondary and tertiary halos!?**

..but no enough data available to substantiate the idea…

@ UA9: Channeling experiments at SPS

A bent crystal should efficiently deflected halo particles away from the beam core toward a downstream massive absorber

The selective and coherent scattering on atomic planes of an aligned Si-crystal replaces the random scattering process on single atoms of an amorphous target

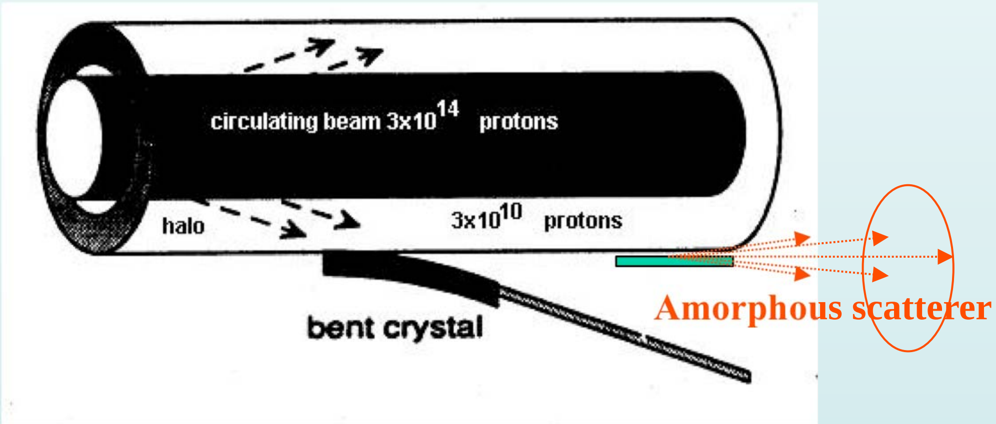

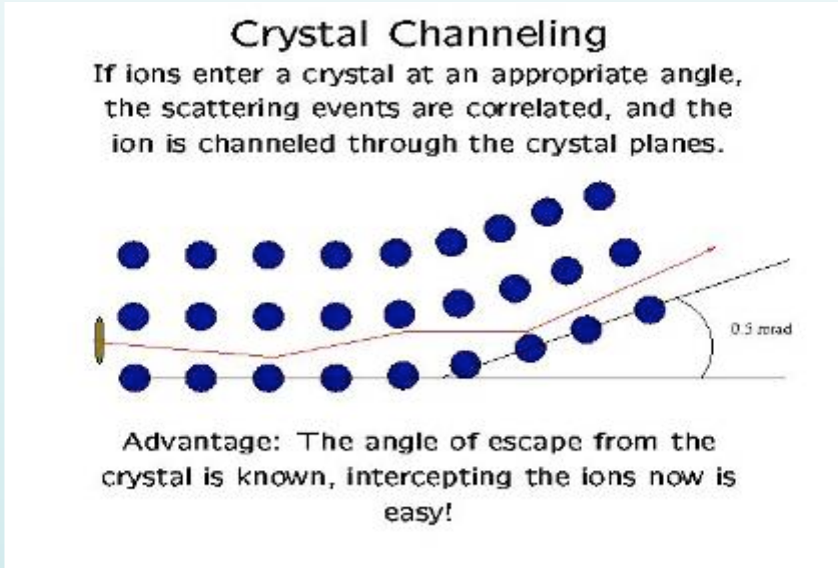

The possible use of crystal for phase II collimation at LHC can be extensively tested at SPS now.

@ First observation: 400 GeV/c CERN, 2006

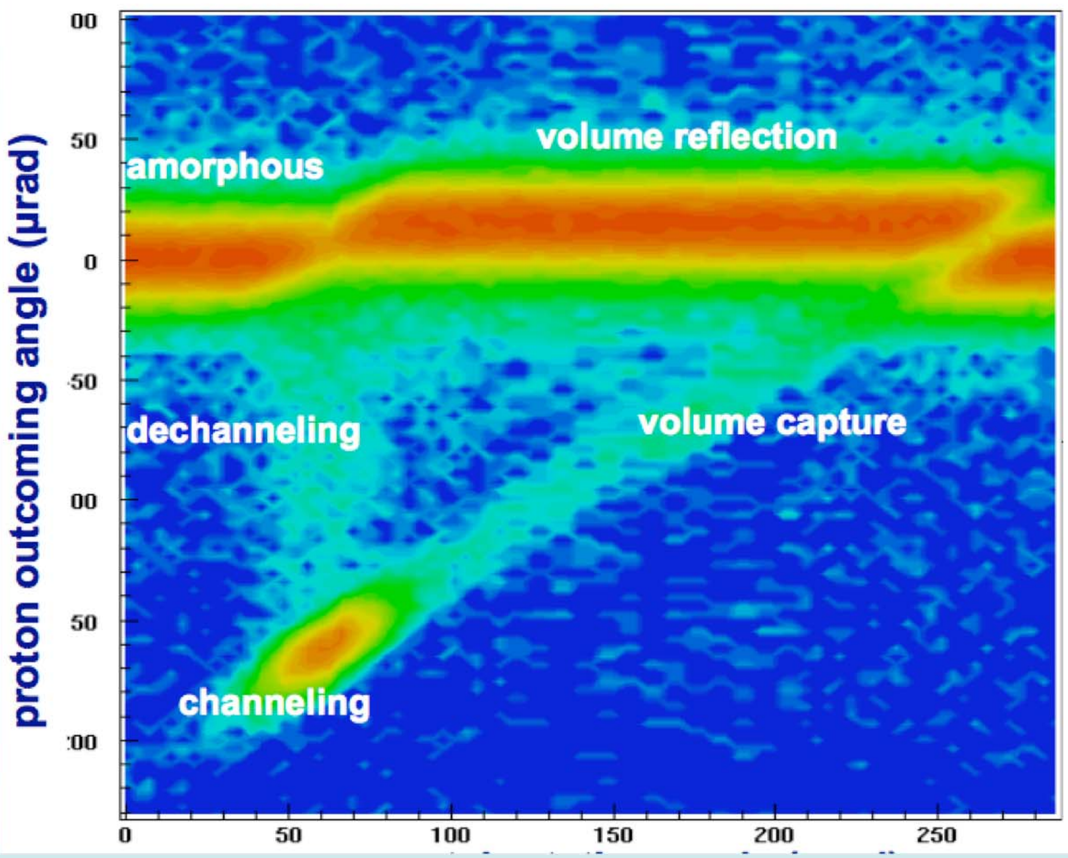

Single strip crystal

- ***First measurement*** **of the volume reflection effect with a proton beam of 400 GeV/c**

EFFICIENCY	VALUE
VOLUME REFLECTION	98.2 ± 0.1%
CHANNELING	51.2 ± 0.7%
VOLUME CAPTURE	1.3 ± 0.1%
DECHANNELING	5.0 ± 0.4%

@ Installation in Crystal Tank at SPS

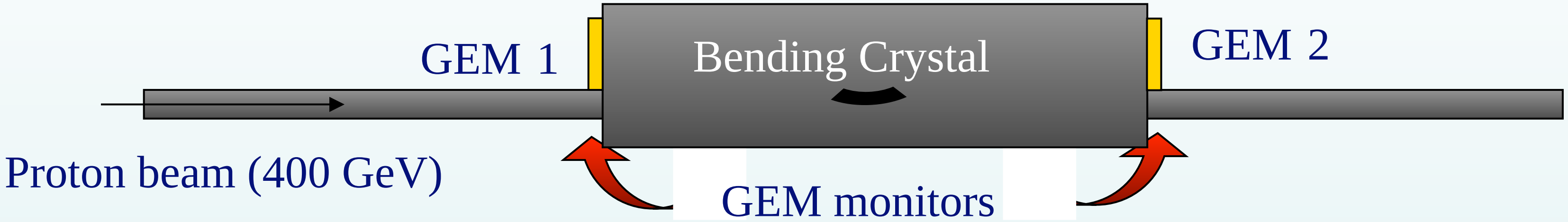

Front view

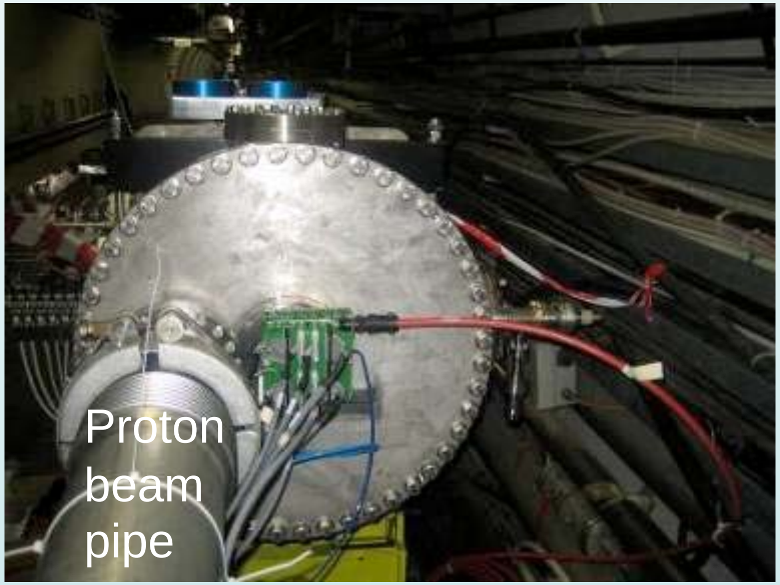

Side view

Contribution of Roma1 and Frascati (February 2009)

The GEM monitors will measure the beam halo during the crystal insertion

@ Beam deflection based on channeling process

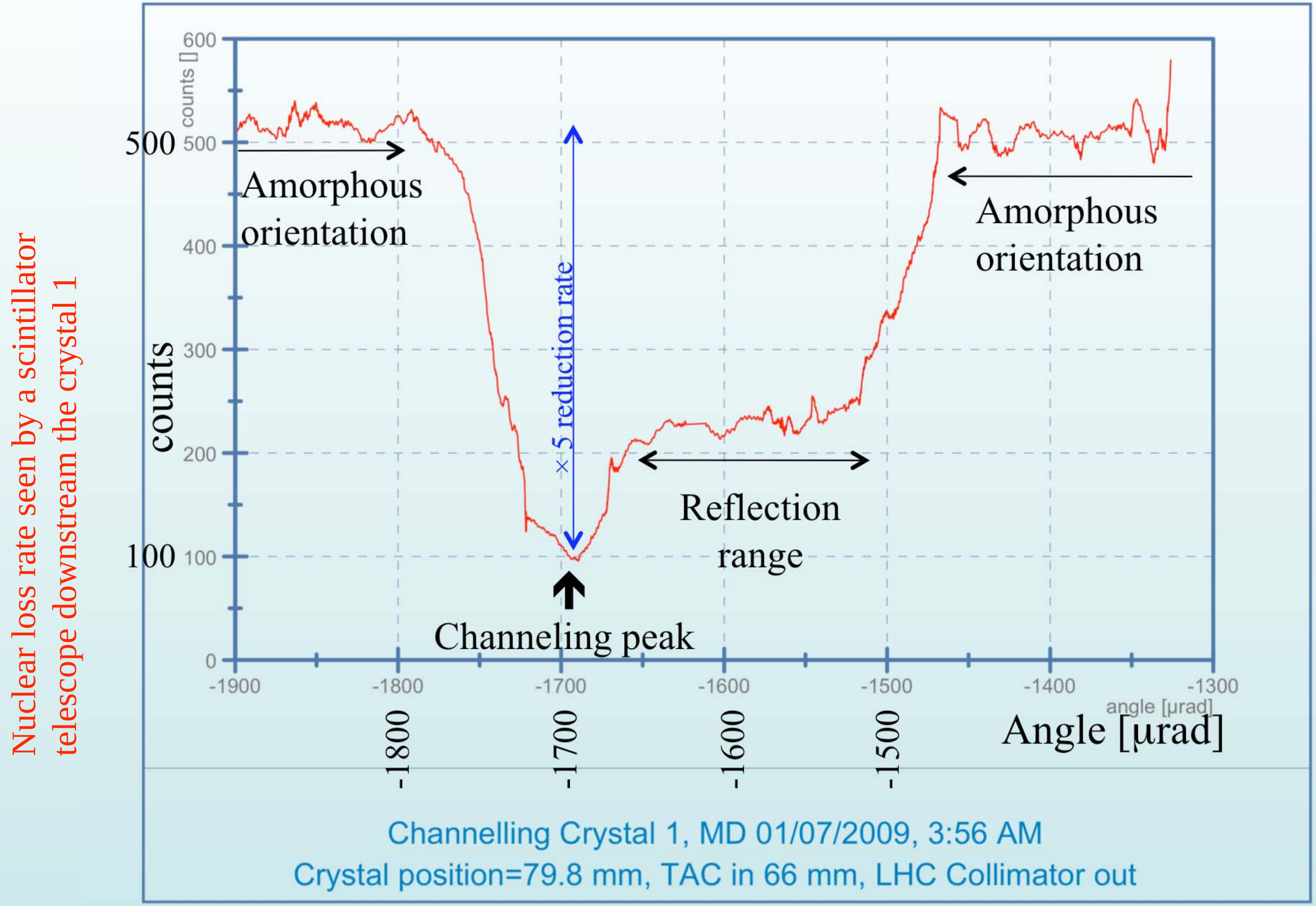

- *Nuclear loss rate* (including diffractive) strongly depressed

@ Deflected beam profile: Medipix

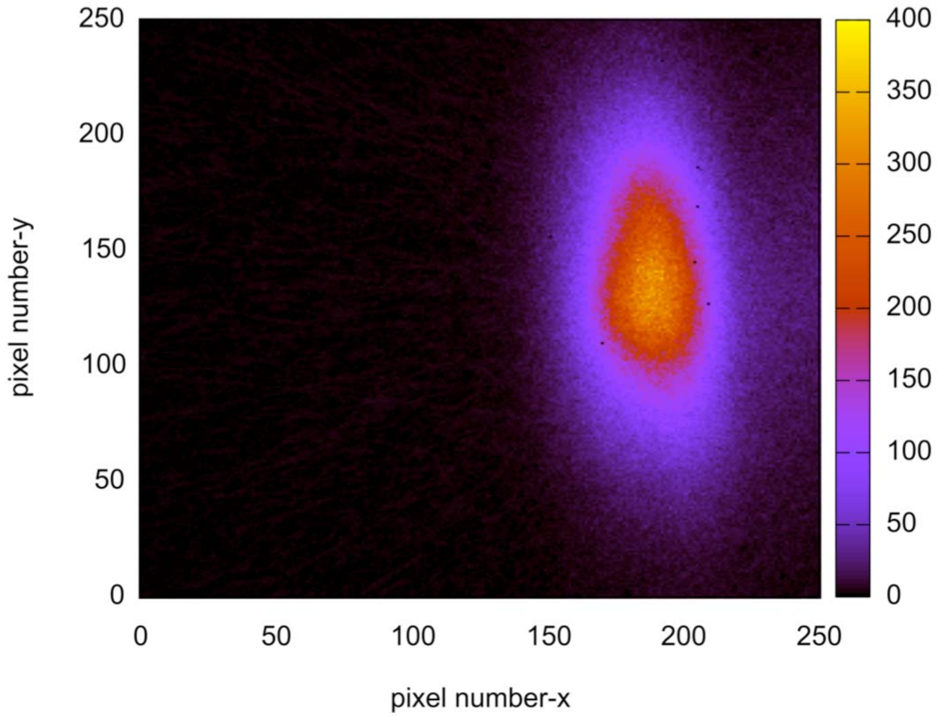

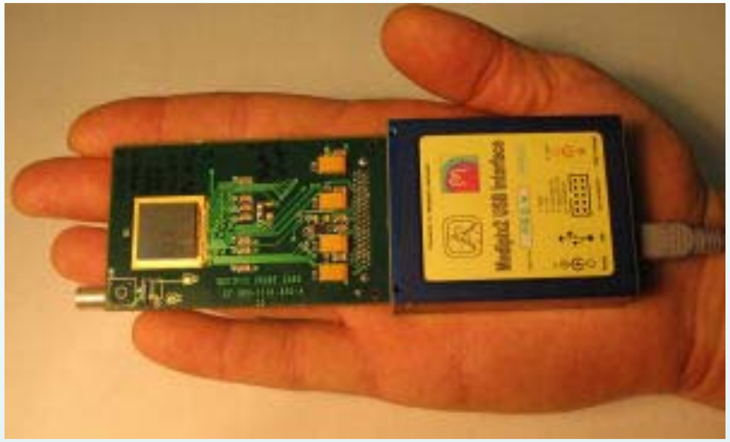

Medipix sensor of the type inserted in the UA9 roman pot,
provided by L. Tlustos (PH/ESE)

- 256×256 square pixels
- 1 pixel size = 55 μm
- 1 frame integration time 1 s

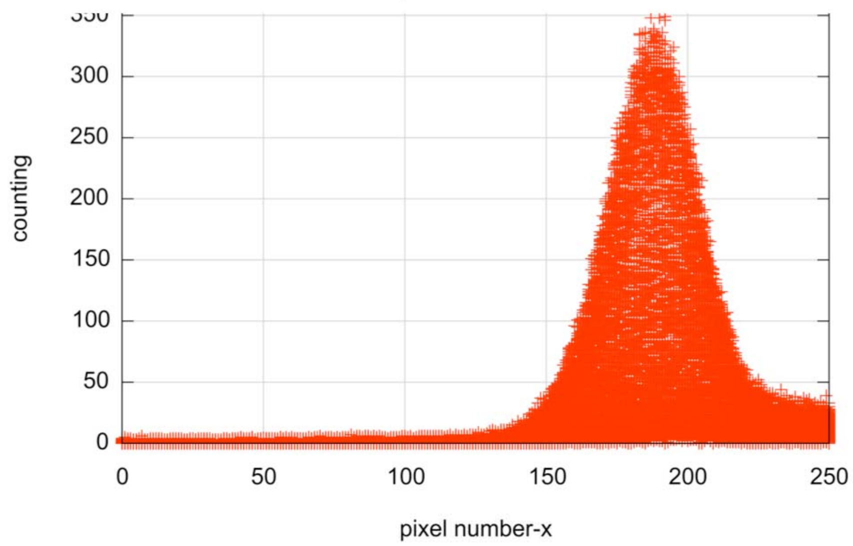

- Pick/valley density ratio = 10
- We observed a ratio of 30 (recording lost for a computer crash)

On X-Ray & Neutron Waveguiding:
…from surface down to bulk channeling…

@ X-ray Optics Problem

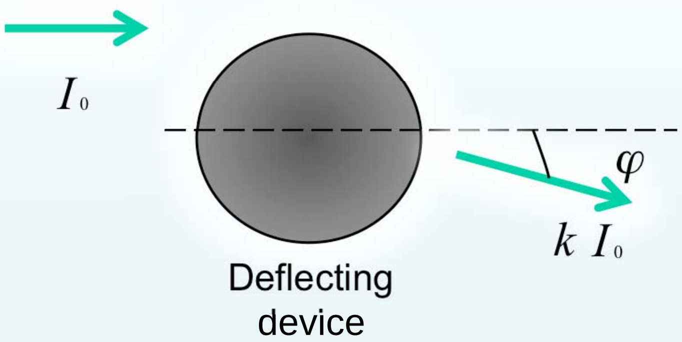

$$k \equiv k(\varphi) << 1$$

$$k_{\max}(\varphi) \propto 0.1 \div 0.2$$

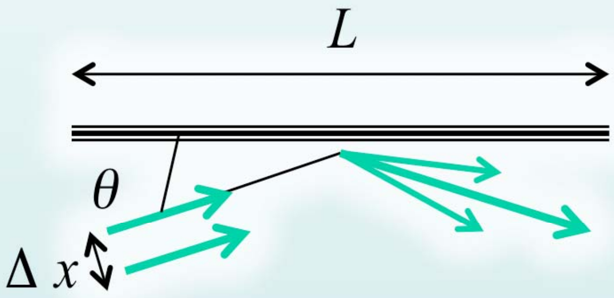

$$\theta << 1 \qquad (\theta \leq \theta_c \equiv \omega_p / \omega)$$

$$k(\theta) \approx 1$$

$$\left.\begin{array}{l} \omega \approx 10\ keV \\ \Delta x \approx 1\ mm \end{array}\right\} \rightarrow \quad \varphi \approx 1^{o} \quad \Rightarrow \quad L \geq \frac{\Delta x\ \varphi}{\theta_c^2} \approx 2\ m$$

The system sizes may be significantly diminished (in about two orders of magnitude) by the use of capillary systems.

@ Basic principles

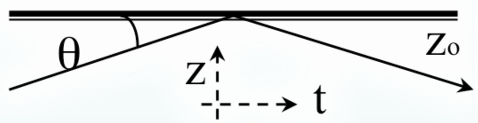

$$\Delta\vec{E} + \varepsilon k^2 \vec{E} = 0$$

$$\varepsilon = \begin{cases} 1, & z \le z_0; \\ 1-\theta_c^{\,2}, & z > z_0 \end{cases}$$

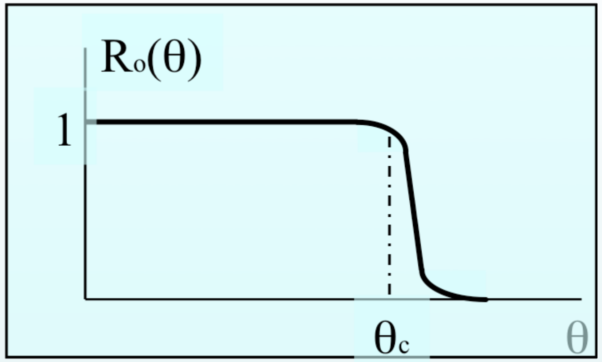

$\theta_c = \omega_p/\omega \approx 30eV/\omega$, $\omega \rightarrow$ photon energy

$\theta \le \theta_c \Rightarrow$ total external reflection (TER)

$$\Delta\theta \approx 2\theta_c$$

$$I \propto \int_{\theta_{\min}}^{\theta_c} R(x)\sin(x)\,dx \propto L^{-1}$$

free space propagation $\rightarrow L^{-2}$

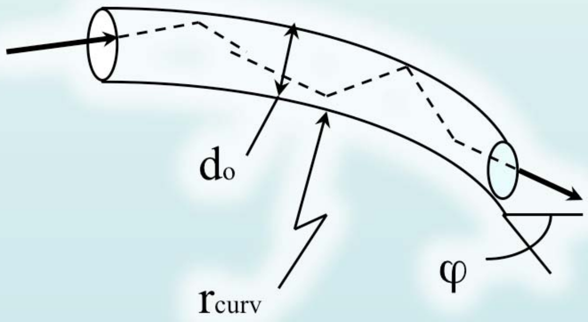

$\theta_i \le \theta_c$ - multiple TER

$\dfrac{r_{curv}\theta_c^{\,2}}{2d_0} \ge 1$ - effective guide

$$I(\varphi) \propto \int [R_0(x)]^{N(x,\varphi)}\,dx$$

@ X-ray and neutron capillary optics

Basic idea of polycapillary optics is very close to the phenomenon of charged particle channeling

@ beam bending through large angles

@ divergent beam to convergent one

@ divergent to quasiparallel & vv

Number of applications

@ scientific instrumentation (XRF, XRD)

@ elemental/structural analysis

@ medicine (diagnostics, therapy)

@ astrophysics

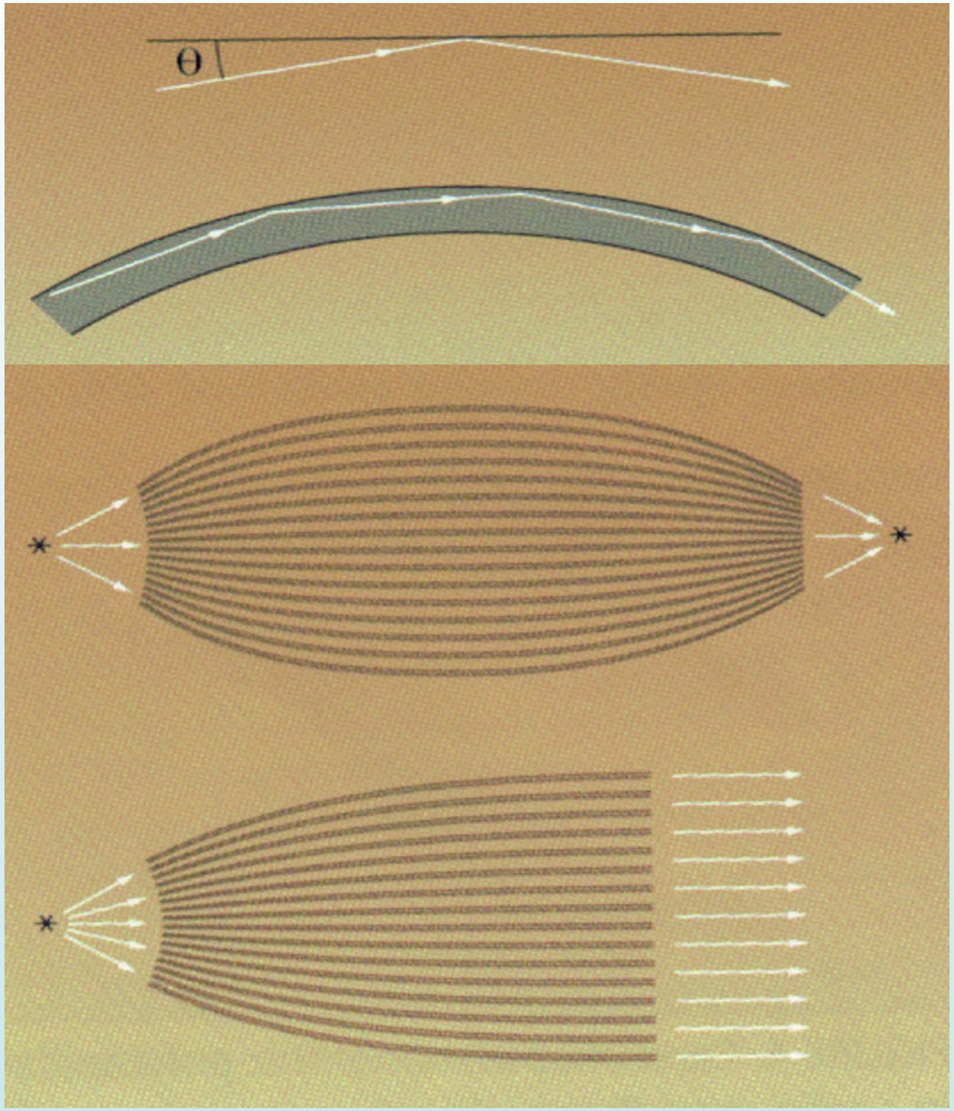

@ Samples of capillary optics

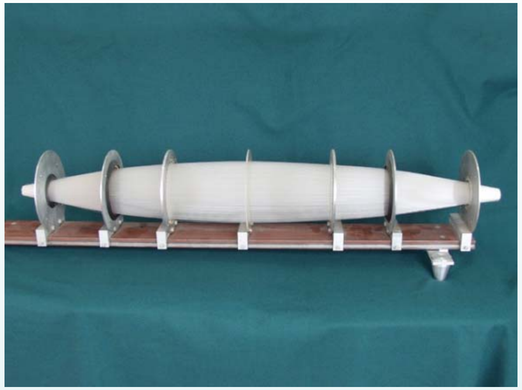

1st generation:
[m]

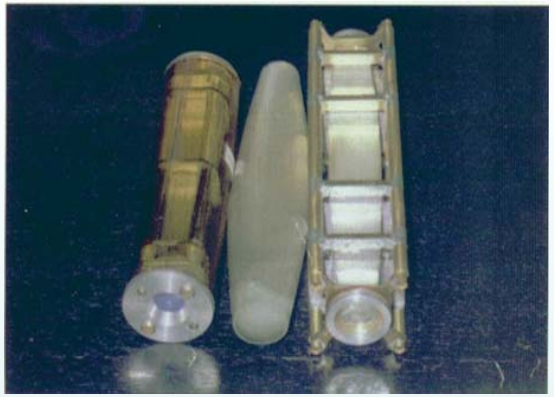

2^{d} generation:
[cm]

3^{d} & 4th generations:
[mm]

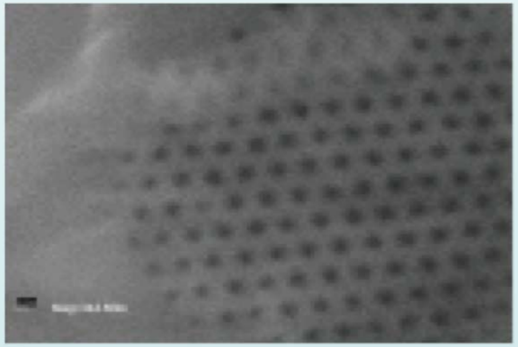

5th generation:
[μm]

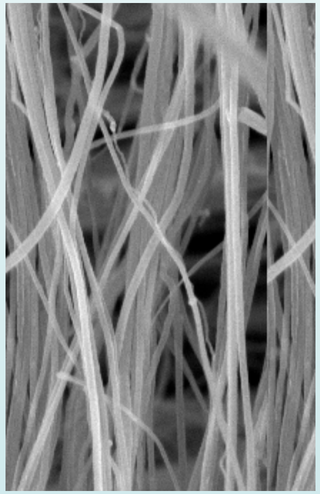

?n-capillaries?

@ polyCO Evolution: "from micro- down to nano"

Generation	Kind of optics	Sizes: length & channel & energy
• 1^{st}	*Assembled lens made of single capillaries*	*1 m & 1 mm & ≤ 10 keV*
• 2^{nd}	*Monolithic lens made of single capillaries*	*10-30 cm & 0.1-1 mm & ≤ 10 keV*
• 3^{rd}	*Assembled lens made of polycapillaries*	*10 cm & 10-50 μm & ≤ 20 keV*
• 4^{th}	*Monolithic lens made of polycapillaries*	*4-10 cm & 1-10 μm & ≤ 50 keV*
• 5^{th}	*Monolithic integral micro lens*	*1-3 cm & 0.3-1 μm & ≤ 100 keV*

Micro-capillaries

Micro → X-rays

Nano → γ-rays (?)

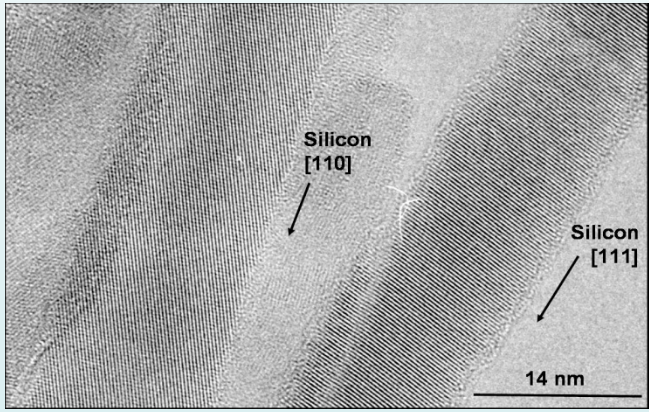

Nanotubes & Nanochannels

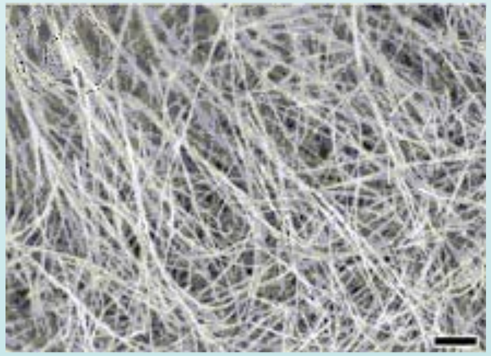

@ Samples of Nanostructures

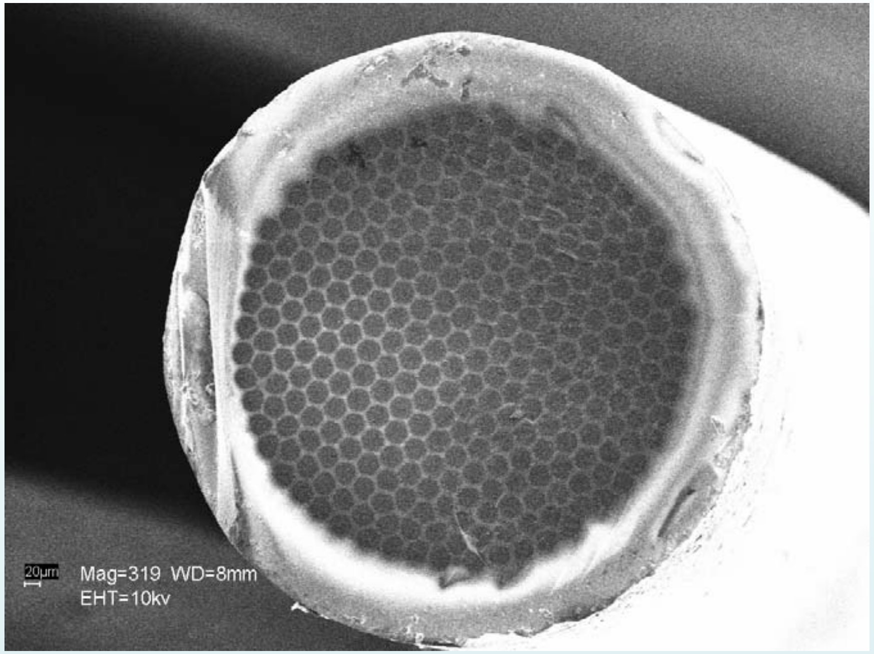

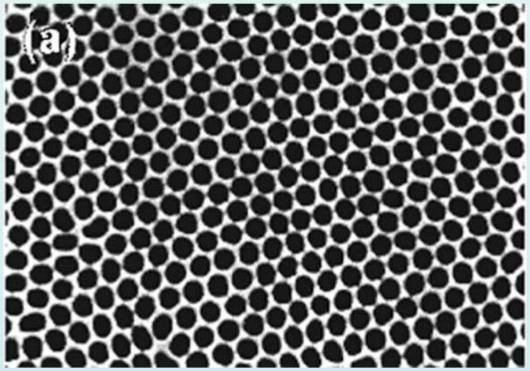

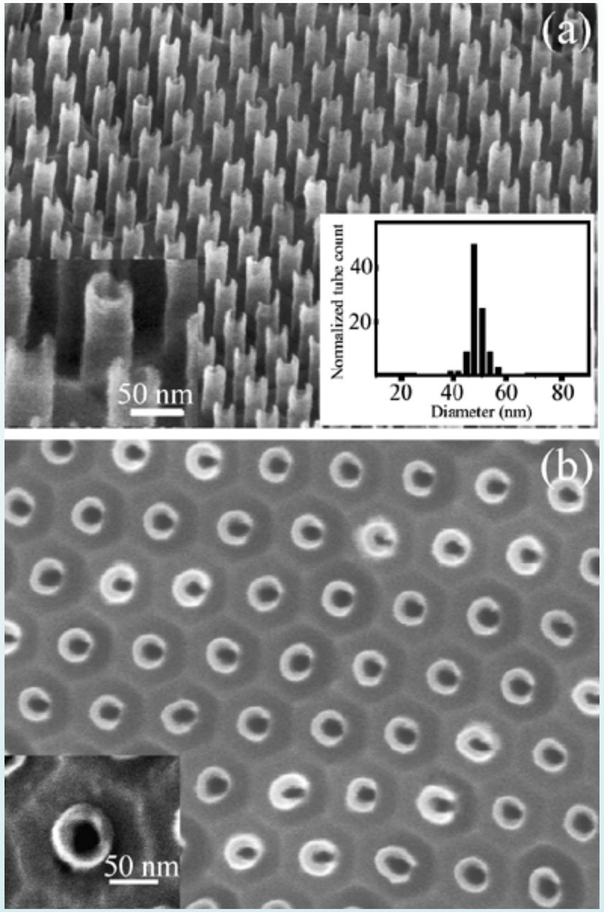

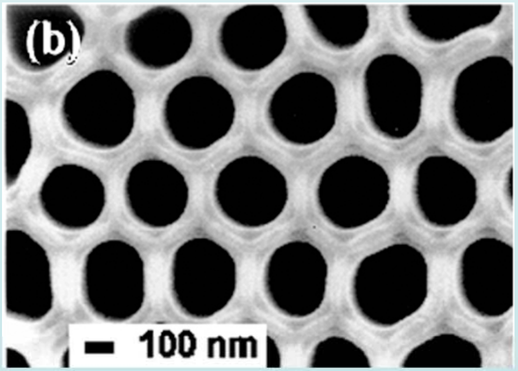

@ Modes of channeling along curved surfaces

$\vec{\mathbf{k}} = (\mathbf{k}_\perp, \mathbf{k}_{||})$

$k_\perp \simeq k\theta \; (\theta < \theta_c)$

$\lambda_\perp = \lambda/\theta >> \lambda$

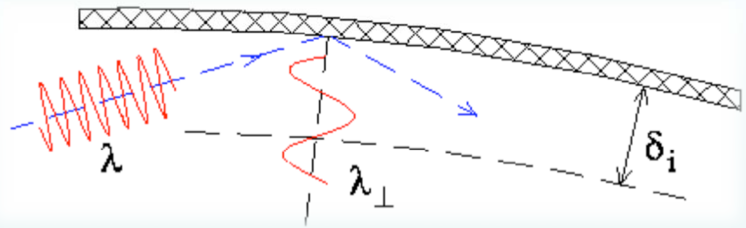

Effective guide channel $\delta_i(\theta) \simeq \lambda_\perp(\theta)$

$$(r_{curv})_i \theta^3 \sim \lambda$$

$(r_{curv})_i = 1\, cm \div 1\, m$

$\theta \simeq 10^{-3} rad$

$\lambda \simeq 0.1 \div 10\ \text{Å}$

Upper limit of the curvature radius

$(r_{curv})_m \sim 10\ cm$

$\lambda \sim 1\ \text{Å}$

Very important expression for the diffraction limit estimation –
can be applied for any kind of the optics:

@ Quantum basics

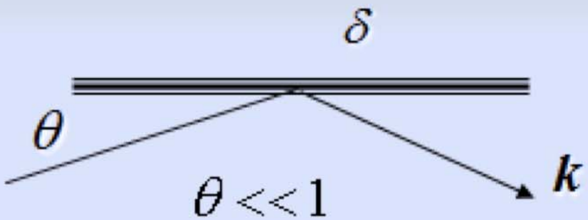

$\theta << 1$

$k_\perp \approx k\theta$

1st order: $\Delta\varepsilon(\vec{r}) = 0$ *- no roughness*

Wave equation:

$$\Big(-\nabla^2 + \underbrace{k^2\delta(\vec{r}_\perp) - k_\perp^{\,2}}_{V_{eff}}\Big)E(\vec{r}_\perp) = 0$$

$$k^2\left(\delta(\vec{r}_\perp) - \theta^2\right) =$$

$$= \underbrace{\begin{cases} -k^2\theta^2, & r_\perp < r_1 \\ k^2\left(\delta_0 - \theta^2\right), & r_\perp \geq r_1 \end{cases}}$$

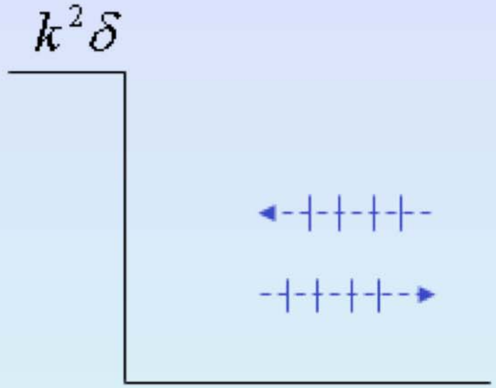

plane (flat) surface

Total external reflection

$$V_{eff} \equiv 0 \Rightarrow \theta_c \equiv \theta \approx \sqrt{\delta_0}$$

@ Quantum basics… *Curvature*

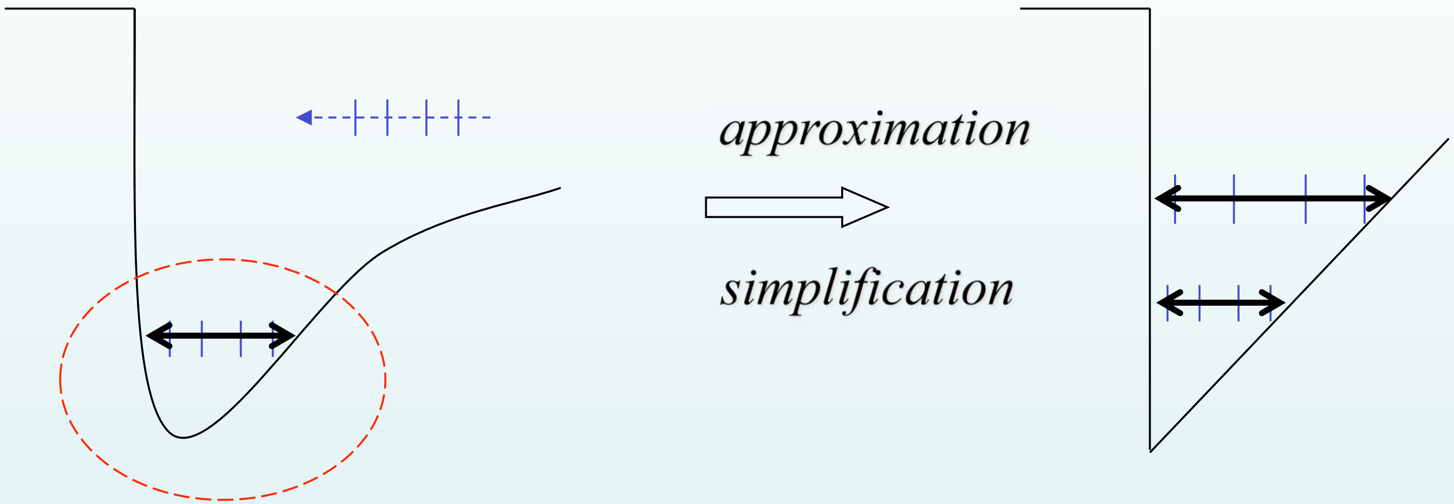

additional term to

$$V_{eff} \longrightarrow 2\frac{-k^2 r_\perp}{r_{curv}}$$

"potential energy": angular momentum of photon

$$k r_{curv} \varphi$$

$$V_{eff} = k^2\left(\delta\left(\vec{r}_\perp\right) - \theta^2 - 2\frac{r_\perp}{r_{curv}}\right)$$

@ Surface channeling - "whispering X gallery"

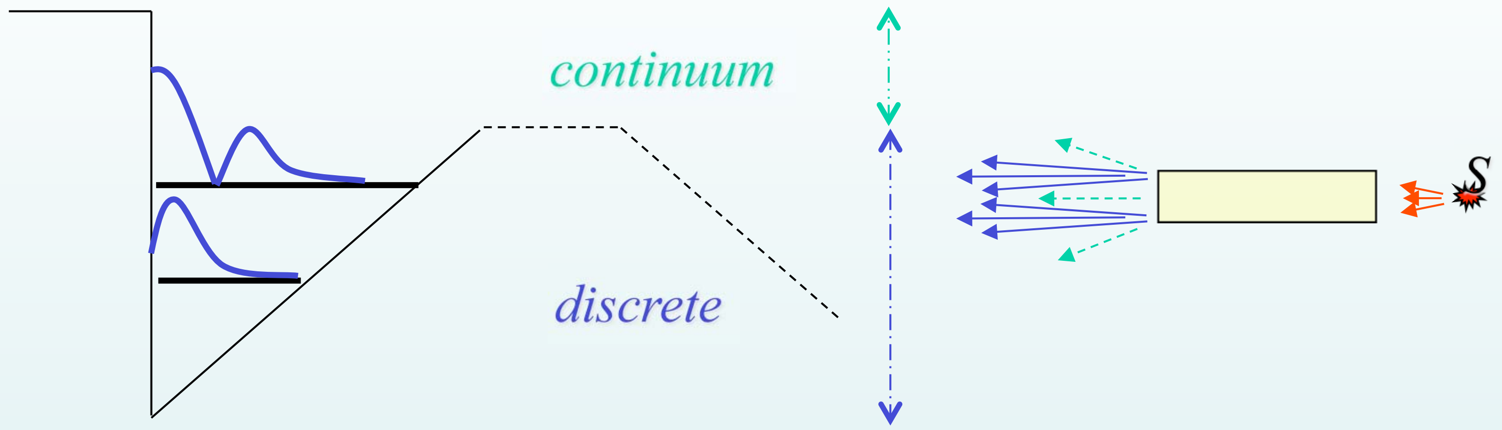

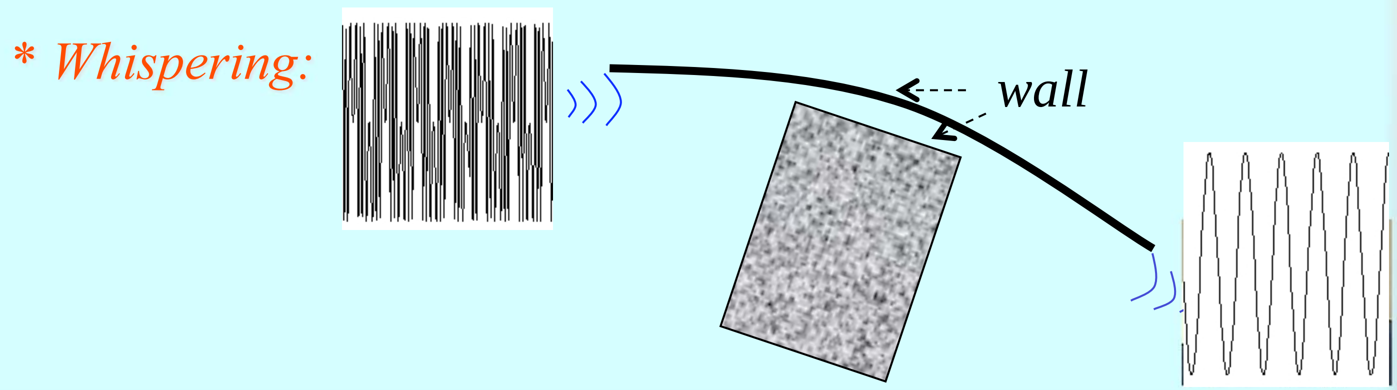

@ Divergence - *surface channeling*

APPLIED PHYSICS LETTERS VOLUME 78, NUMBER 19 7 MAY 2001

Divergence behavior due to surface channeling in capillary optics

G. Cappuccio
CNR—Istituto di Strutturistica Chimica, P.O. Box 10, I-00016 Montelibretti Sc., Italy and INFN—Laboratori Nazionali di Frascati, P.O. Box 13, I-00044 Frascati, Italy

S. B. Dabagov[a)]
INFN—Laboratori Nazionali di Frascati, P.O. Box 13, I-00044 Frascati, Italy and RAS—P.N. Lebedev Physical Institute, 117924 Moscow, Russia

C. Gramaccioni and A. Pifferi
CNR—Istituto di Strutturistica Chimica, P.O. Box 10, I-00016 Montelibretti Sc., Italy

(Received 21 November 2000; accepted for publication 7 March 2001)

Recent studies on the transmitting and focusing properties of capillary optical systems have shown that several unexpected effects take place during the experiments. One such effect is a dec the beam divergence behind the capillary structures. In this letter, we present results c scattering at grazing angles inside capillaries. During x-ray propagation in capillary channe is a strong angular redistribution of the beam, which has been explained in the framewor wave scattering theory. © *2001 American Institute of Physics.* [DOI: 10.1063/1.137011

Today, based on a 10W x-ray tube, developed in-house and combined with optics, we have created an x-ray source producing quasi-parallel monochromatic flux of $10^{10} \sim 10^{11}$ photons/sec•mm^2, which we have used in diffraction studies.

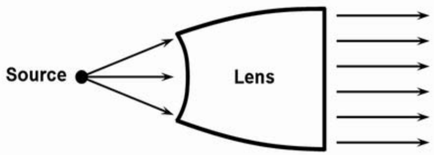

Parallel Beam. Divergence is (2-3)•10^{-3} radian ;
Parallel nature in both directions

Such flux compares well with that usually obtained at synchrotron stations (see Comparison Table 1).

Hence, this system has been named a Laboratory "Synchrotron"

At the same time, in contrast to works carried out at workstations in synchrotron centers where the researchers are strictly limited in time and have other restrains, in our case we provide for a freedom of creativity and possibility of careful and long term investigations.

It should be also taken into consideration that our Laboratory Synchrotron has a reasonable price and is affordable to a great number of scientists, engineers, research laboratories, universities, companies and so on.

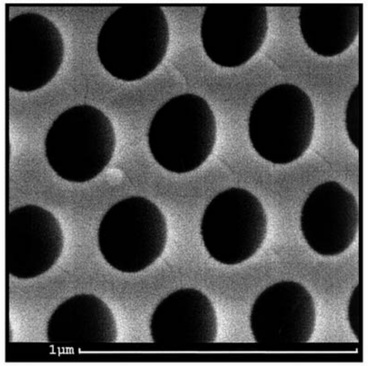

Our Laboratory "Synchrotron" is a portable instrument and does not need special premises, or radiation protection measures.

In addition, it can be easily incorporated in existent diffractometers, which is another advantage of our system.

@ Capillary optics: applications/new portable instruments

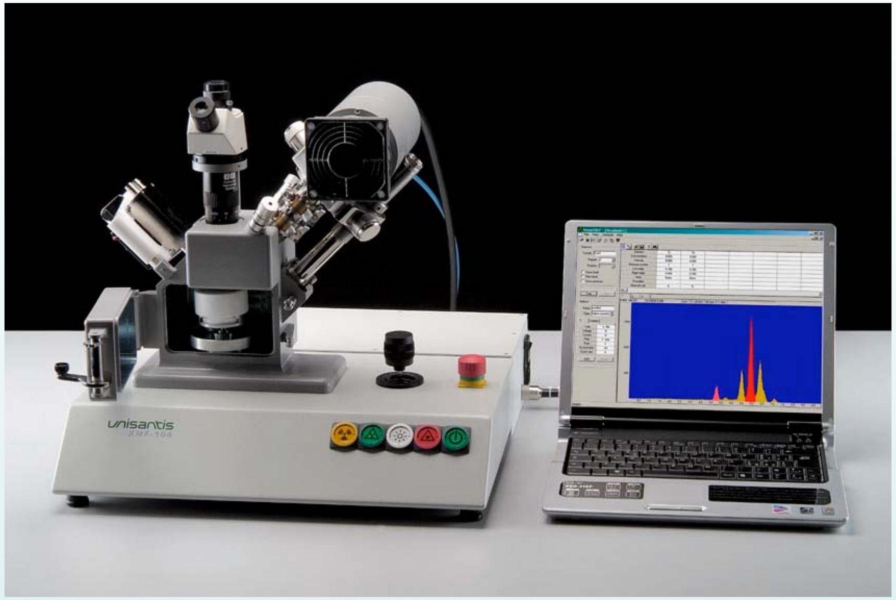

@ Table-top X-Ray Source

→ "Laboratory Synchrotron"

	X12-C NLSL	FOP (ESRF)	ANKA	**UNISANTIS**
Energy Range	8-13 keV	7-21 keV	4-20 keV	**8 keV**
Beam Size	0.3H x 0.5V mm	0.3 x 0.3 mm		**20 to 300 micron**
Beam Divergence	2 mrad			**2-4 mrad**
Flux	~5 x 10^{10} photon / sec (0.3x0.5mm^2)	~5 x 10^{10} photon / sec (0.3x0.3 mm^2)	~1 x 10^{12} photon / sec (mm^2)	**10^{10} - 10^{11} monochromatic photon / sec (mm^2)**
Source Power	Synchrotron (2.6 GeV, 300 mA)	Synchrotron (2.6 GeV, 300 mA)	Synchrotron (2.6 GeV, 300 mA)	**(3÷30) W x-ray tube**

@ Comparison of Various X-ray Micro-Focus Sources

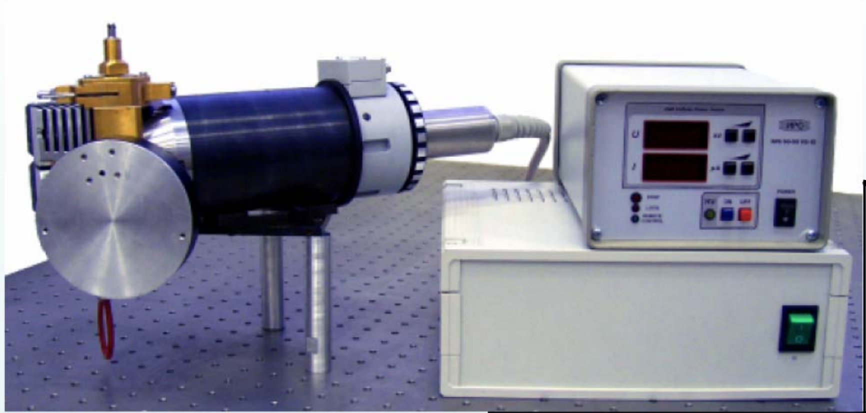

	Osmic	Bruker	Unisantis
Source Power, W	30	24	(3÷30)
Optics	Multi-layer	Focus Mirror	PolyCO
Flux, Cu Kα ph/s/mm^2	≈ 1.9 x 10^9	10^9	10^{10} ÷10^{12}

Maximum power - 50 W
Maximum anode voltage - 50 kV
Material of the anode - Cu, Mo
The size of a tube focal spot ≤ 20 μm

Beams parameters: semilens

Diameter of a beam - 0,1-1 mm
Radiation flux - 10^{10} ph/s/mm^2
Divergence of a beam - 4 mrad Cu; 2 mrad Mo

Beams parameters: full lens

Diameter of a focal spot - 10-50 μm
Radiation flux - 10^{12} ph/s/mm^2
Focus length of a lens - 2-10 mm.

@ PolyCAD

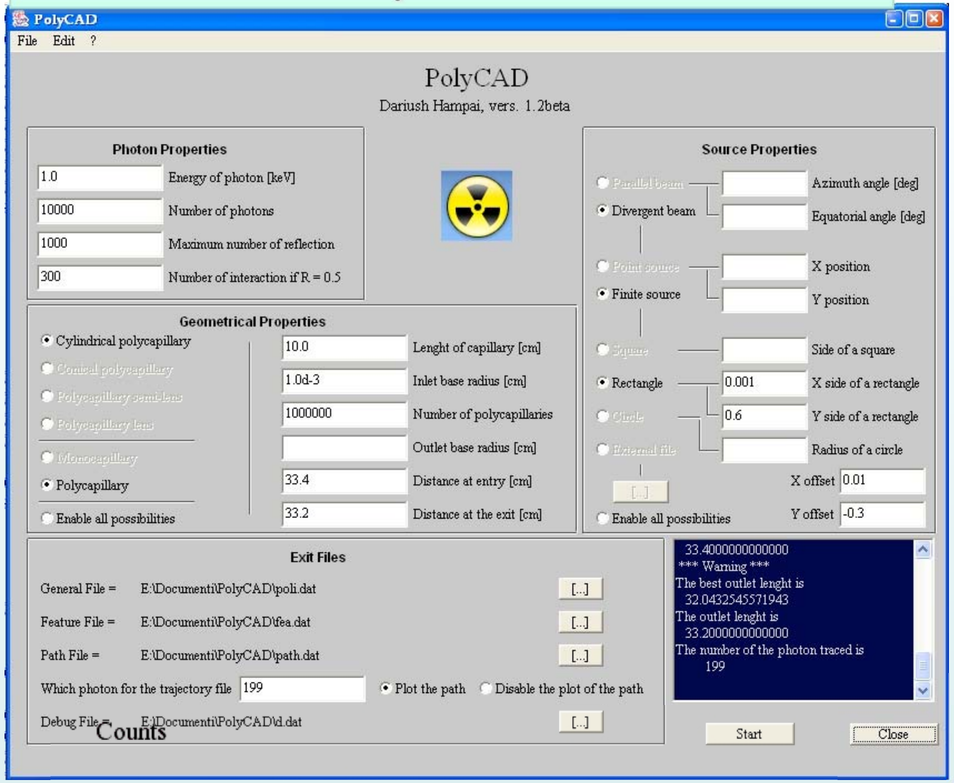
PolyCAD
File Edit ?
PolyCAD
Dariush Hampai, vers. 1.2beta
Photon Properties
1.0 Energy of photon [keV]
10000 Number of photons
1000 Maximum number of reflection
300 Number of interaction if R = 0.5
Source Properties
Parallel beam
Divergent beam
Azimuth angle [deg]
Equatorial angle [deg]
Point source
Finite source
X position
Y position
Square
Rectangle
Circle
External file
Side of a square
0.001 X side of a rectangle
0.6 Y side of a rectangle
Radius of a circle
X offset 0.01
Y offset -0.3
Enable all possibilities
Geometrical Properties
Cylindrical polycapillary
Conical polycapillary
Polycapillary semi-lens
Polycapillary lens
Monocapillary
Polycapillary
Enable all possibilities
10.0 Lenght of capillary [cm]
1.0d-3 Inlet base radius [cm]
1000000 Number of polycapillaries
Outlet base radius [cm]
33.4 Distance at entry [cm]
33.2 Distance at the exit [cm]
Exit Files
General File = E:\Documenti\PolyCAD\poli.dat
Feature File = E:\Documenti\PolyCAD\fea.dat
Path File = E:\Documenti\PolyCAD\path.dat
Which photon for the trajectory file 199
Plot the path
Disable the plot of the path
Debug File = E:\Documenti\PolyCAD\d.dat
33.4000000000000
*** Warning ***
The best outlet lenght is
32.0432545571943
The outlet lenght is
33.2000000000000
The number of the photon traced is
199
Start
Close

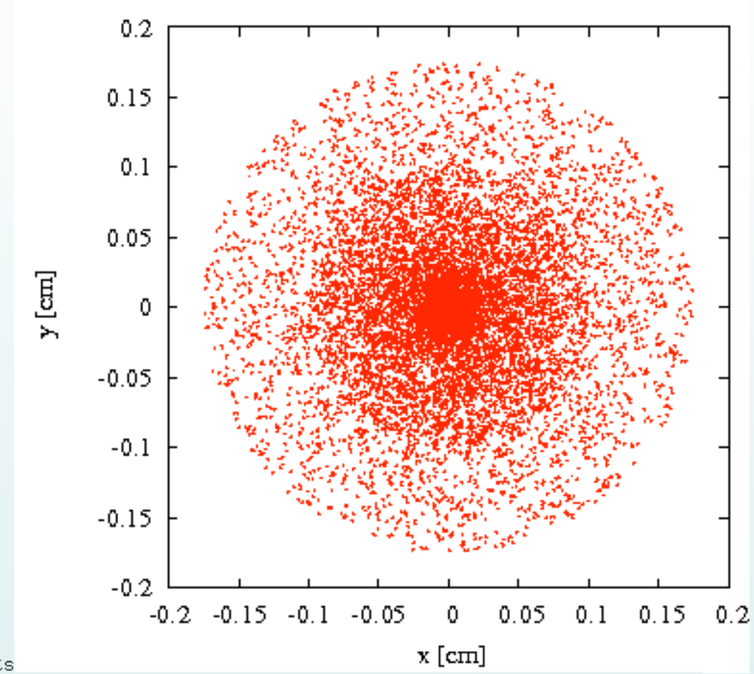
0.2
0.15
0.1
0.05
0
-0.05
-0.1
-0.15
-0.2
y [cm]
-0.2 -0.15 -0.1 -0.05 0 0.05 0.1 0.15 0.2
x [cm]

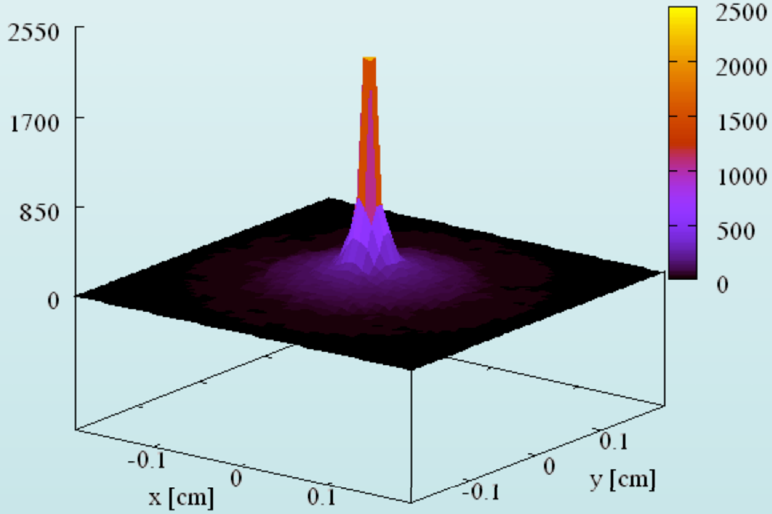
Counts
2550
1700
850
0
2500
2000
1500
1000
500
0
-0.1
0
0.1
x [cm]
-0.1
0
0.1
y [cm]

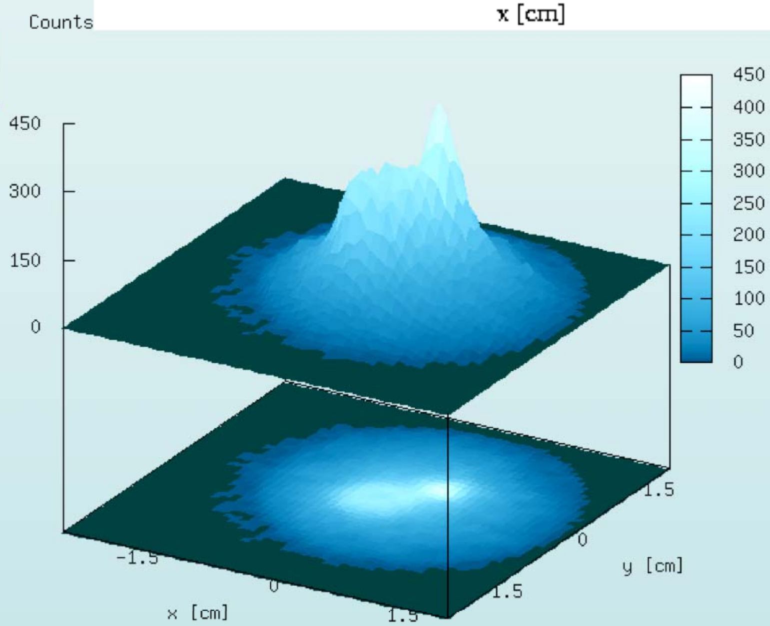
Counts
450
300
150
0
450
400
350
300
250
200
150
100
50
0
-1.5
0
1.5
x [cm]
1.5
0
y [cm]

@ 3D Source - *PolyCAD*

- Reconstruction of the 3D intensity distributions beyond a cylindrical polycapillary due to a couple of X-ray spherical source

- The main peaks are located at the coniugate points respect to each sphere position

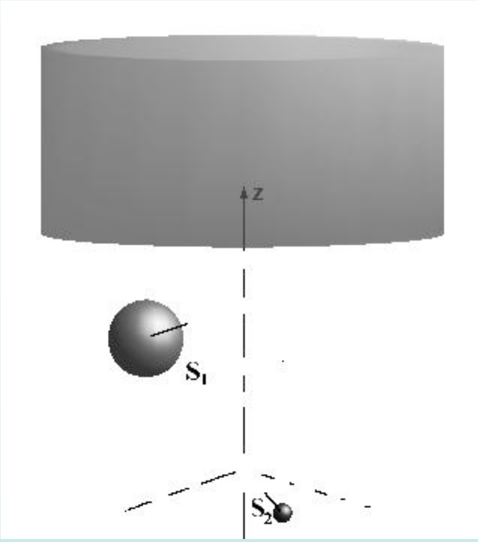

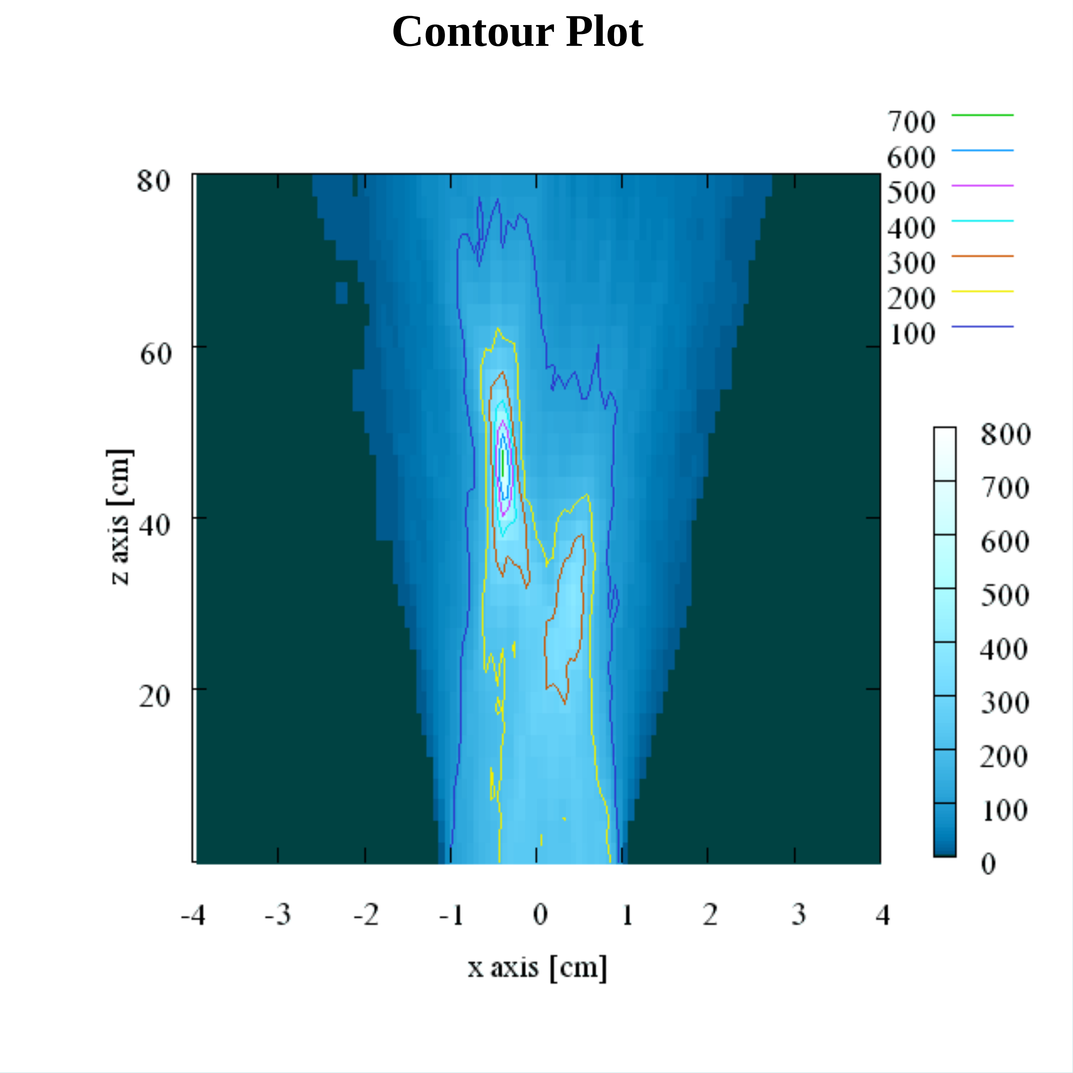

@ Rendering - *PolyCAD*

PolyCAD – Monte-Carlo simulation code for any kind of capillary optical systems

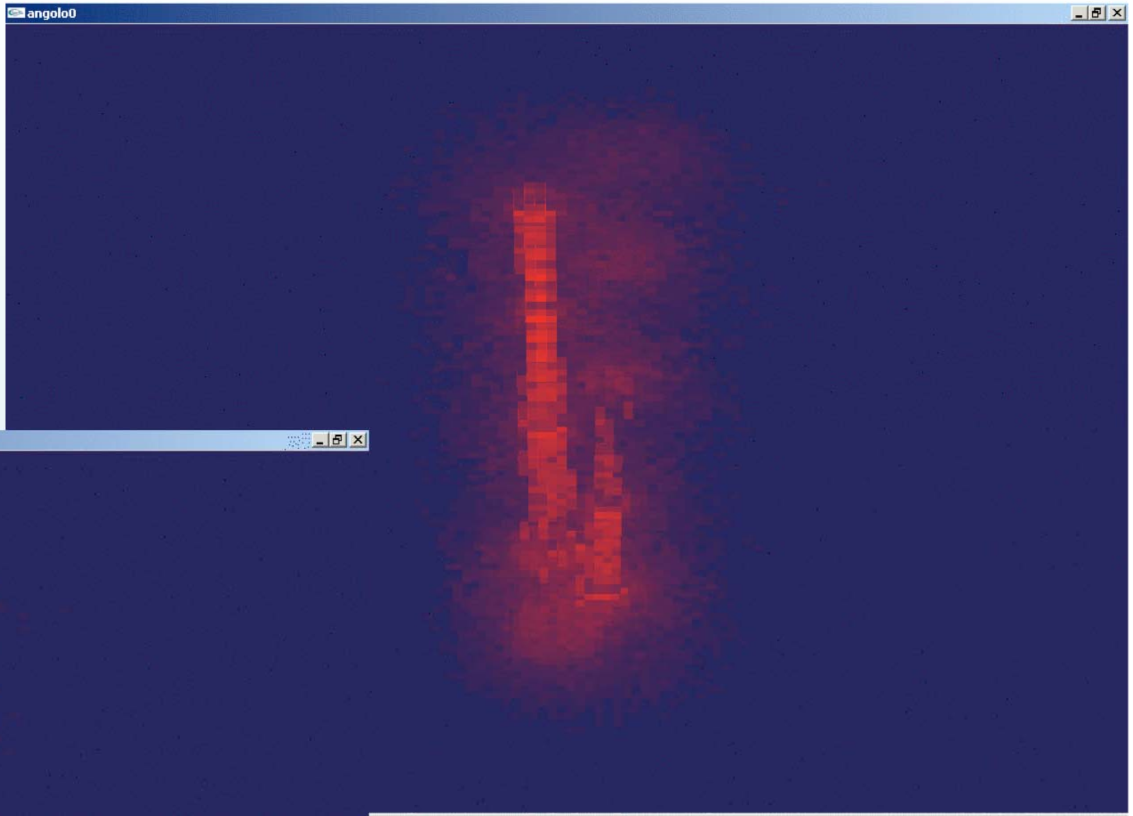

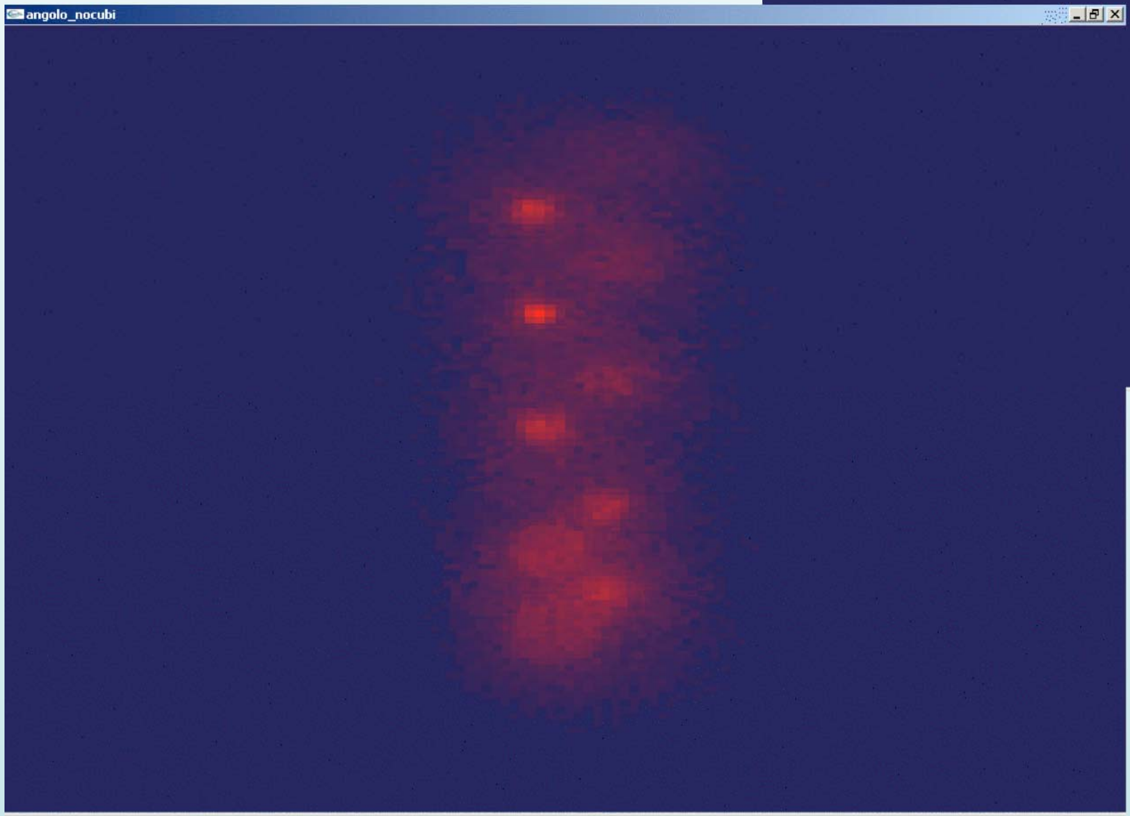

@ X-Lab: Collaboration LNF – UNISANTIS

There is a capability of compressing the electron flux to (1-3) micron at less power.

In case of reflection anode, the power of (40-50) watt can be focused to a (10-15) micron focal spot.

In this instance, anode would be at a 1 mm distance from the window.

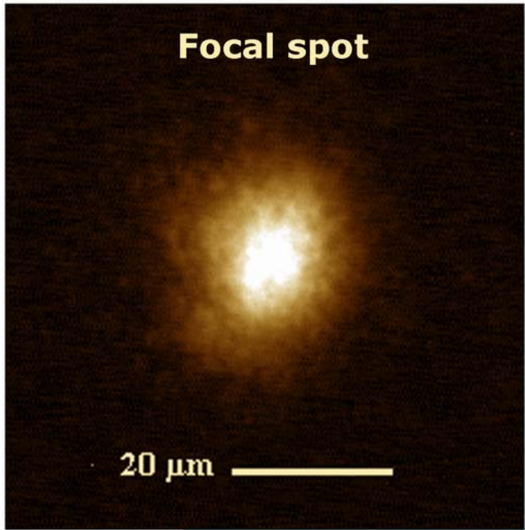

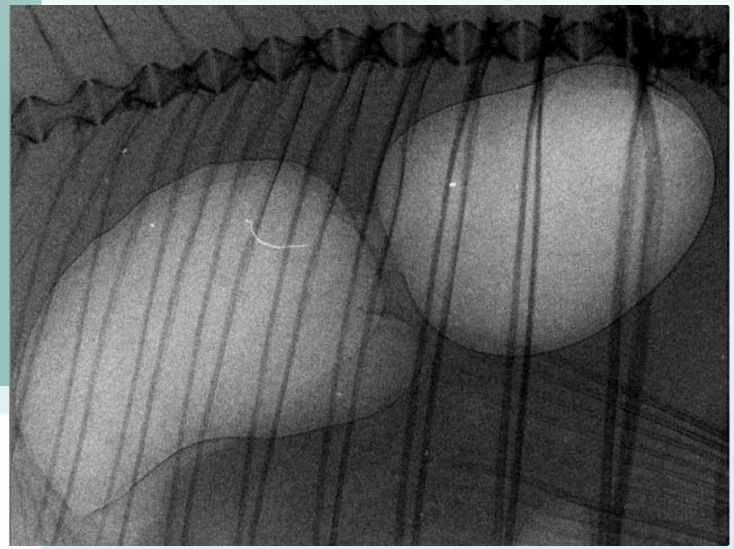

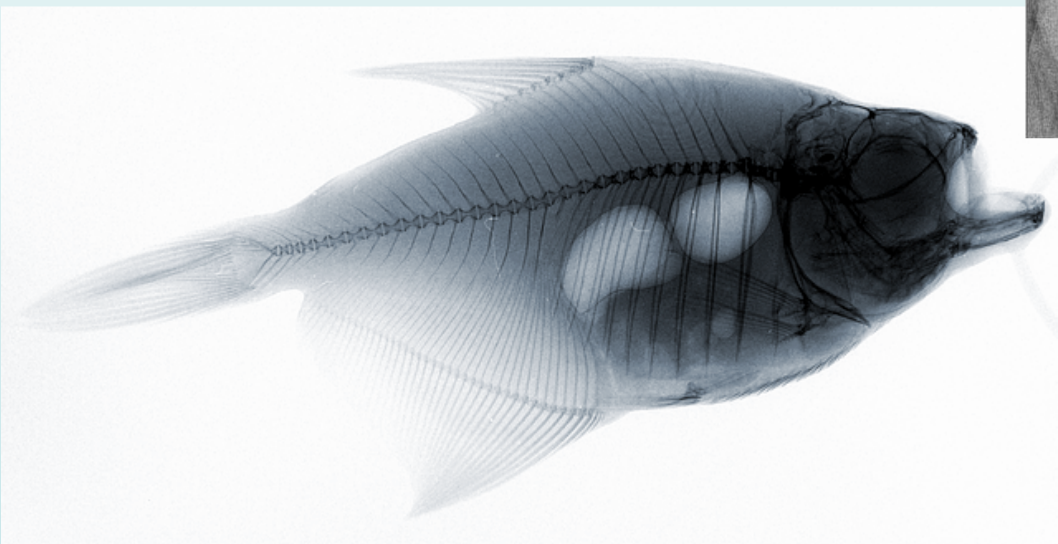

@ X-ray μ-scope: 1st option

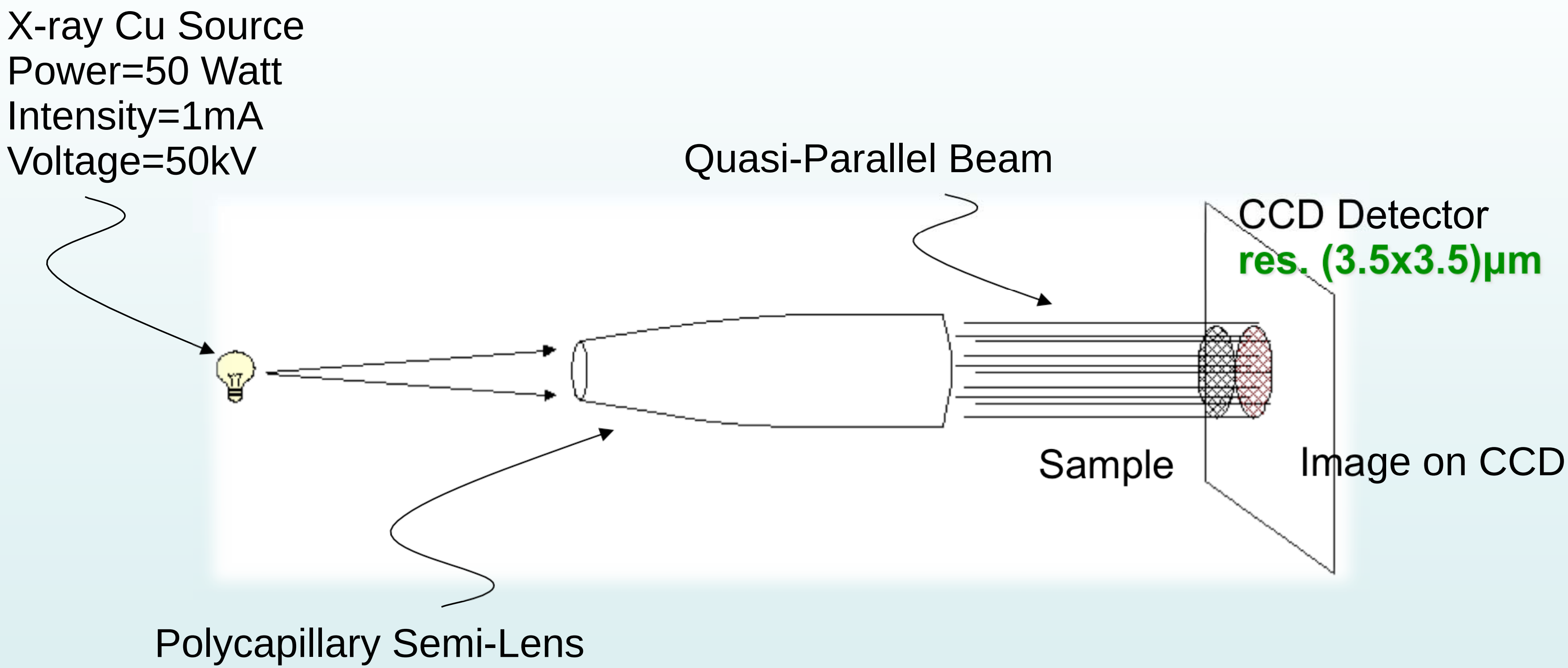

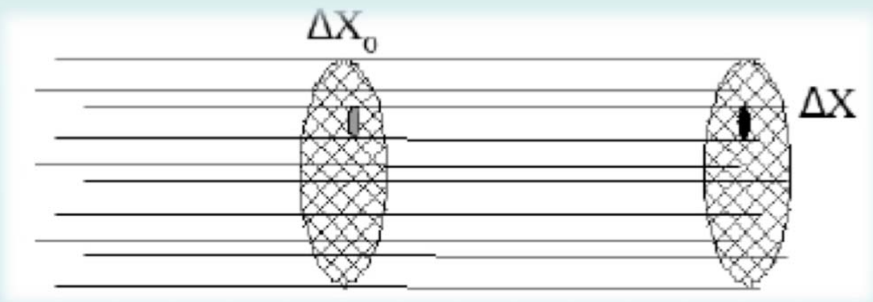

$$|\Delta X - \Delta X_0| \propto l \cdot \Delta\theta$$

l – “sample-detector” distance;
Δθ - residual divergence behind the optics

@ Polycapillary Semilens

- Input focal distance (mm) = 52.7
- Residual Divergence (mrad) ~ 1.
- Transmission ~ 60%

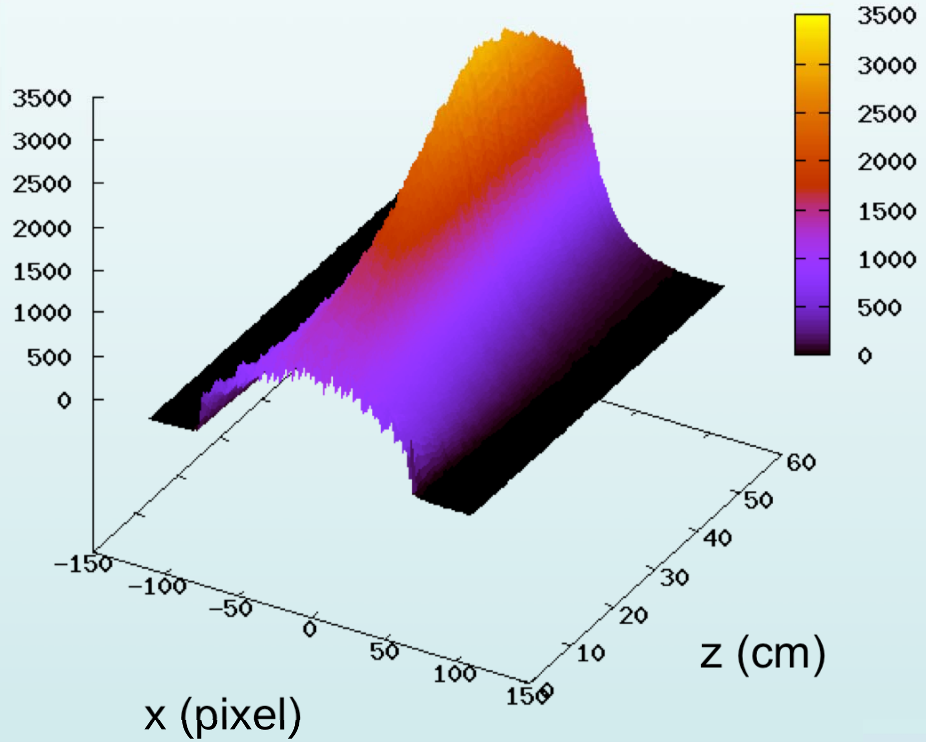

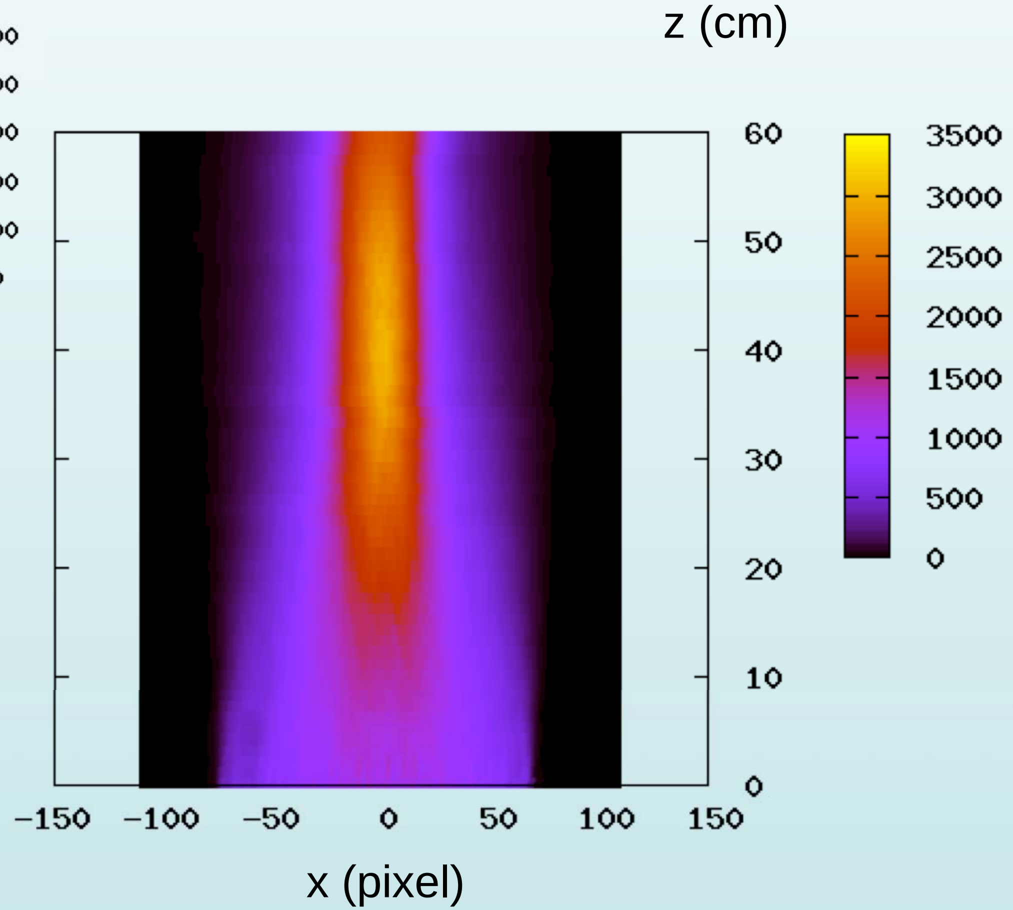

@ High Resolution Image: Cu 400 mesh

- Hole Width 37μm
- Bar Width 25μm

polycapillary pillar

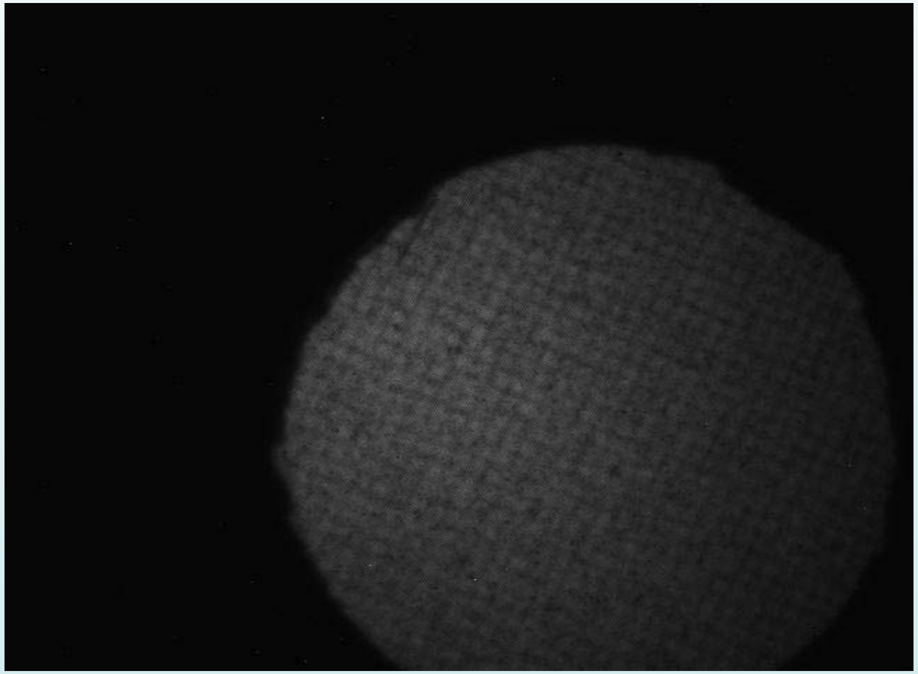

23 cm Polycapillary – CCD Detector

@ High Resolution Image: Au 1000 mesh

- Hole Width 19μm
- Bar Width 6μm

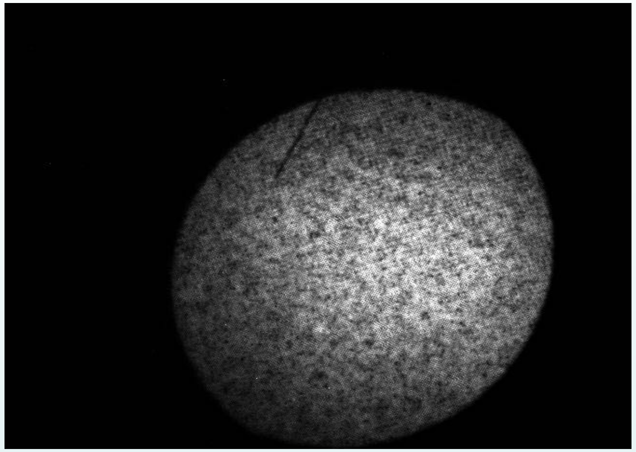

23 cm optics – CCD

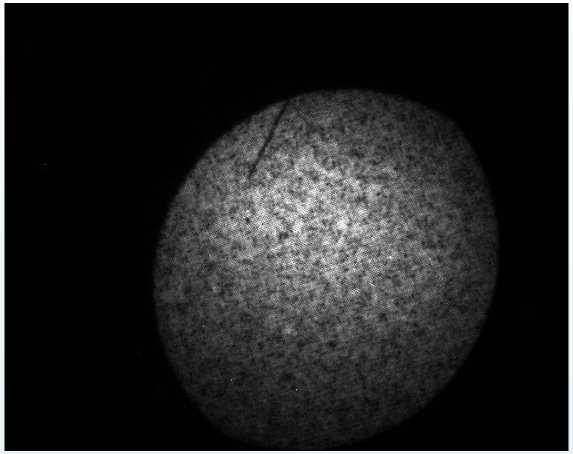

44 cm optics – CCD

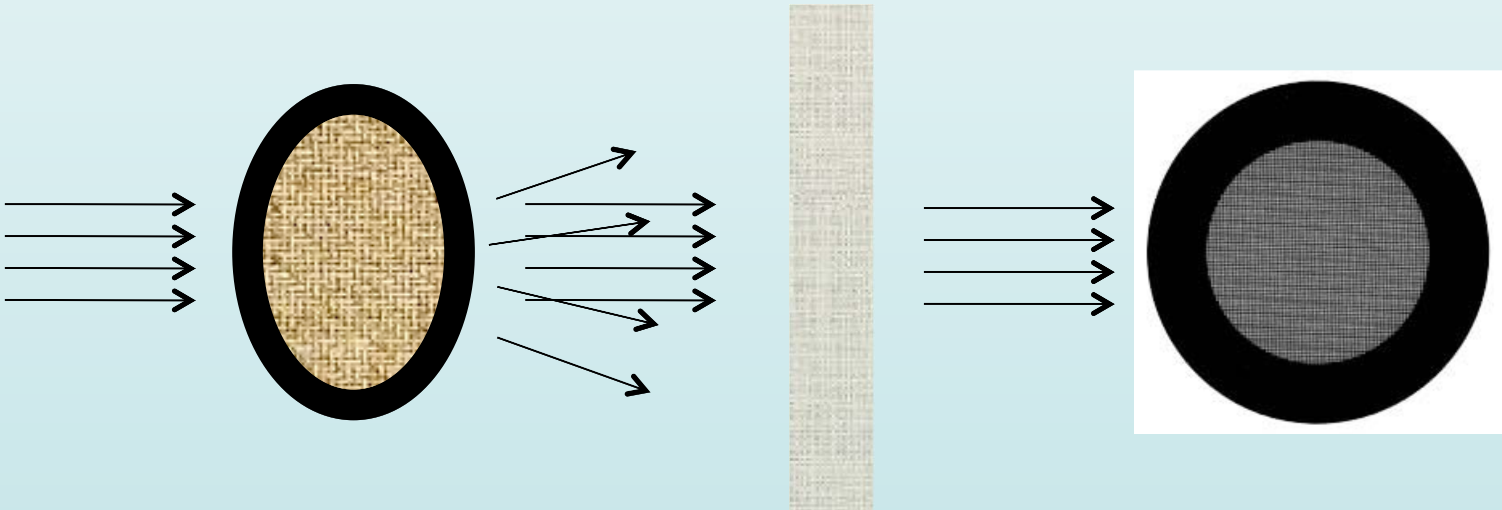

@ High Resolution Image: Chips

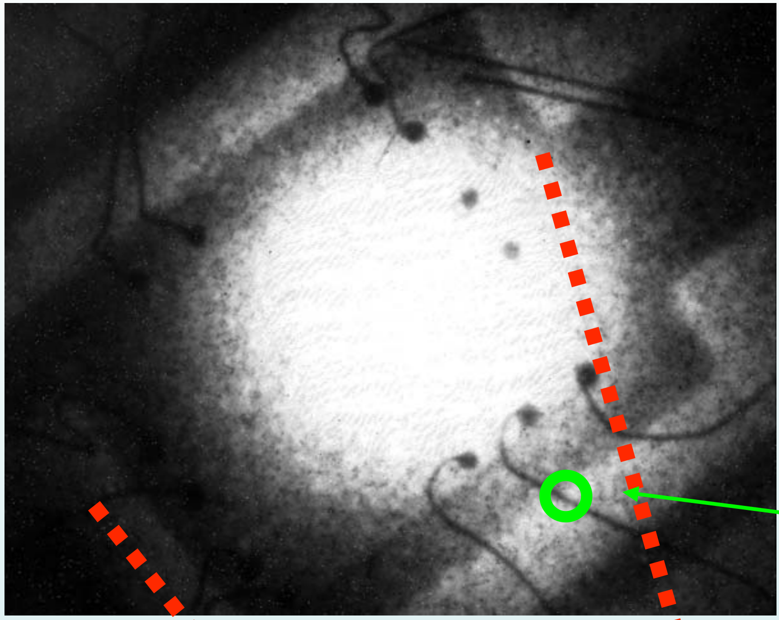

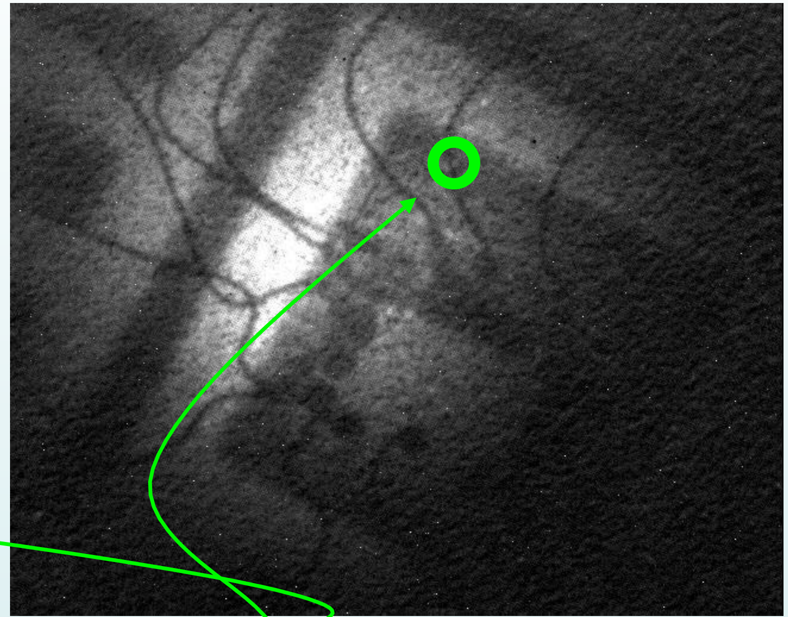

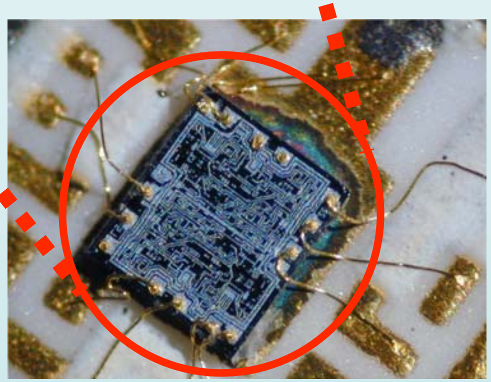

Gold Wires ~ 25 μm

@ Collaboration: LNF – UNISANTIS

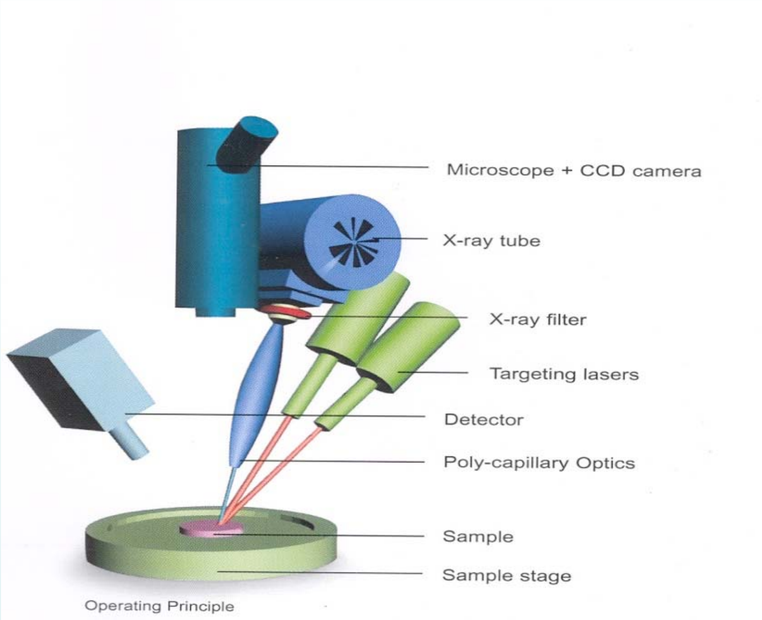

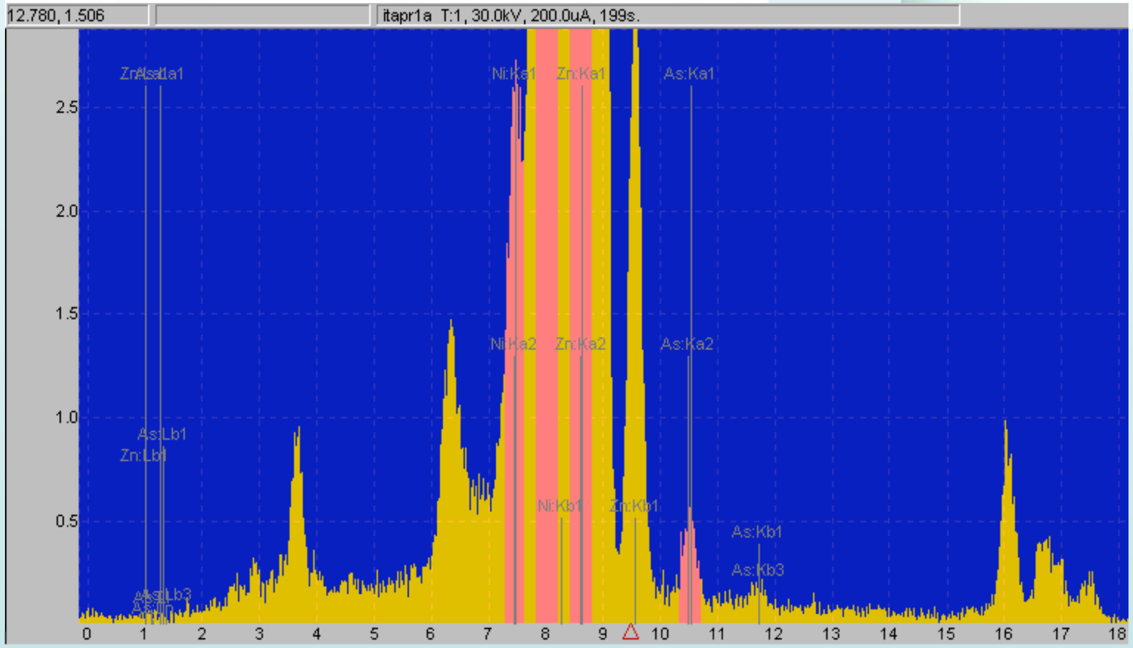

Alloy from Sample copper ancient archeological dig and spectrum of this alloy obtained using this micro analyzer (13 Century, Italy).

@ μXRF mapping (i)

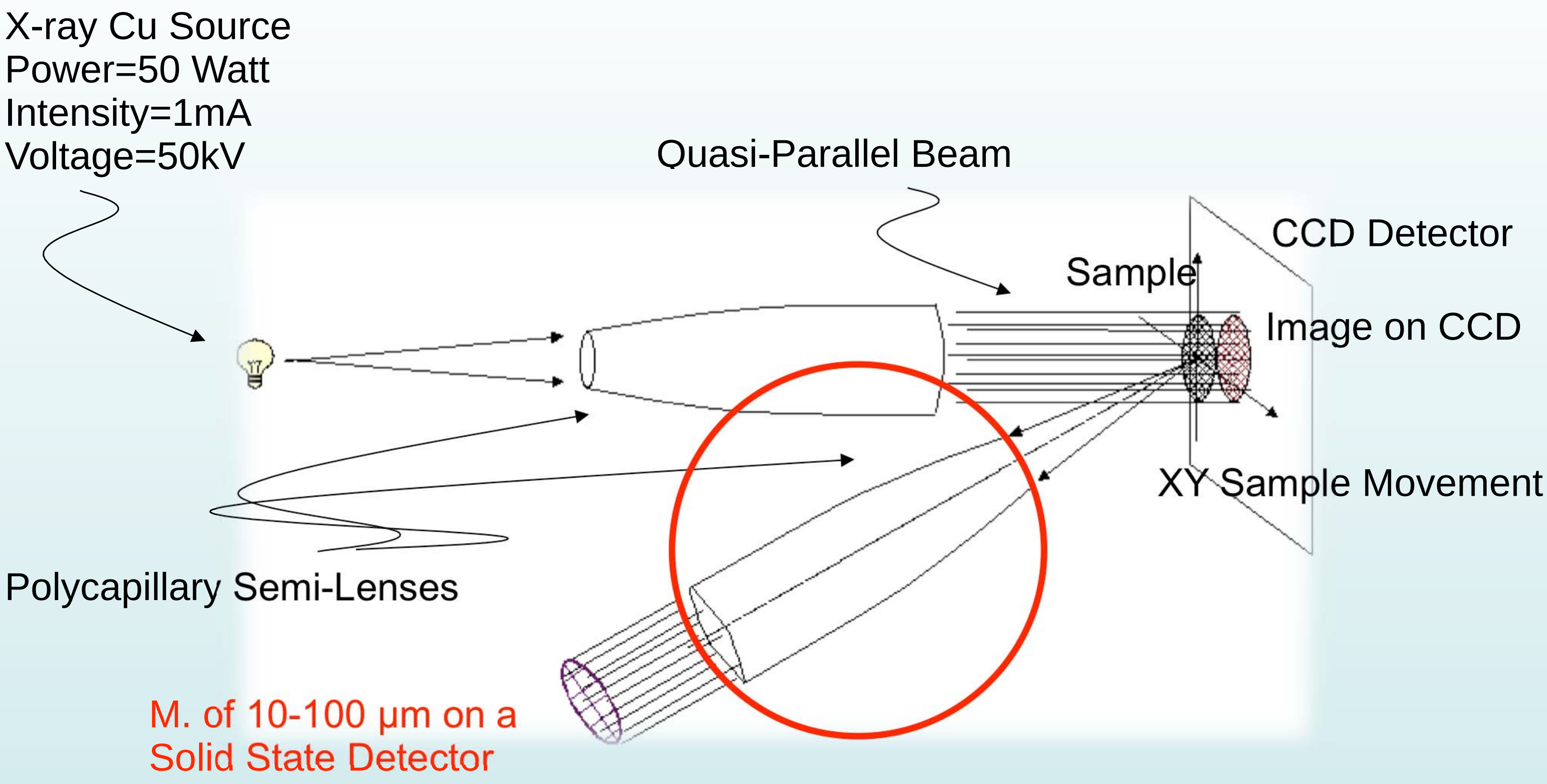

@ μXRF mapping (ii)

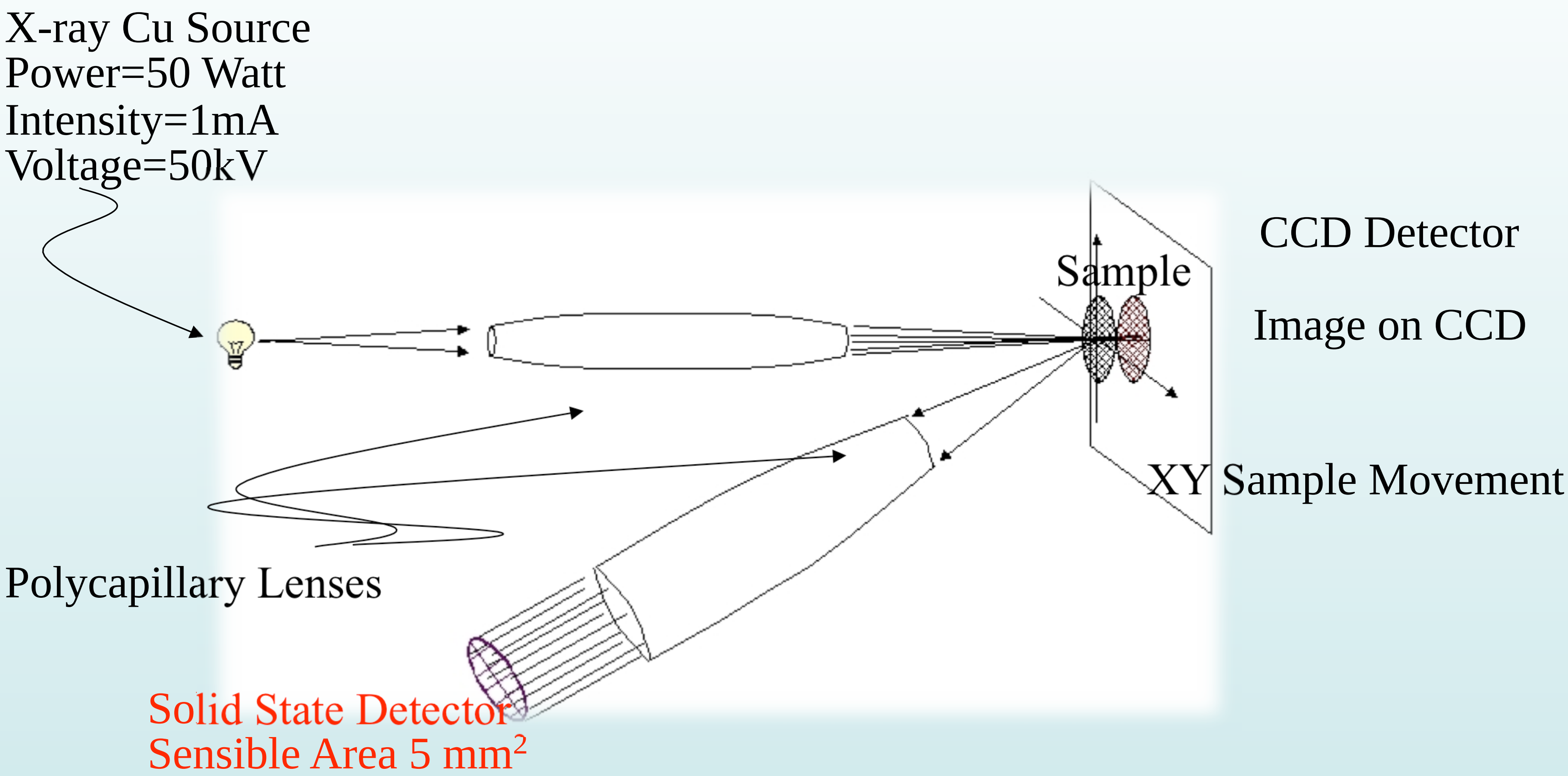

@ μXRF mapping on Fe_2O_3

μXRF Mapping – 200x200 μm^2 spot
4x4 mm^2 measured area (40x40 steps)
2 minutes for each spot
CuKα Tube; V=24 KV, I=0.750 mA

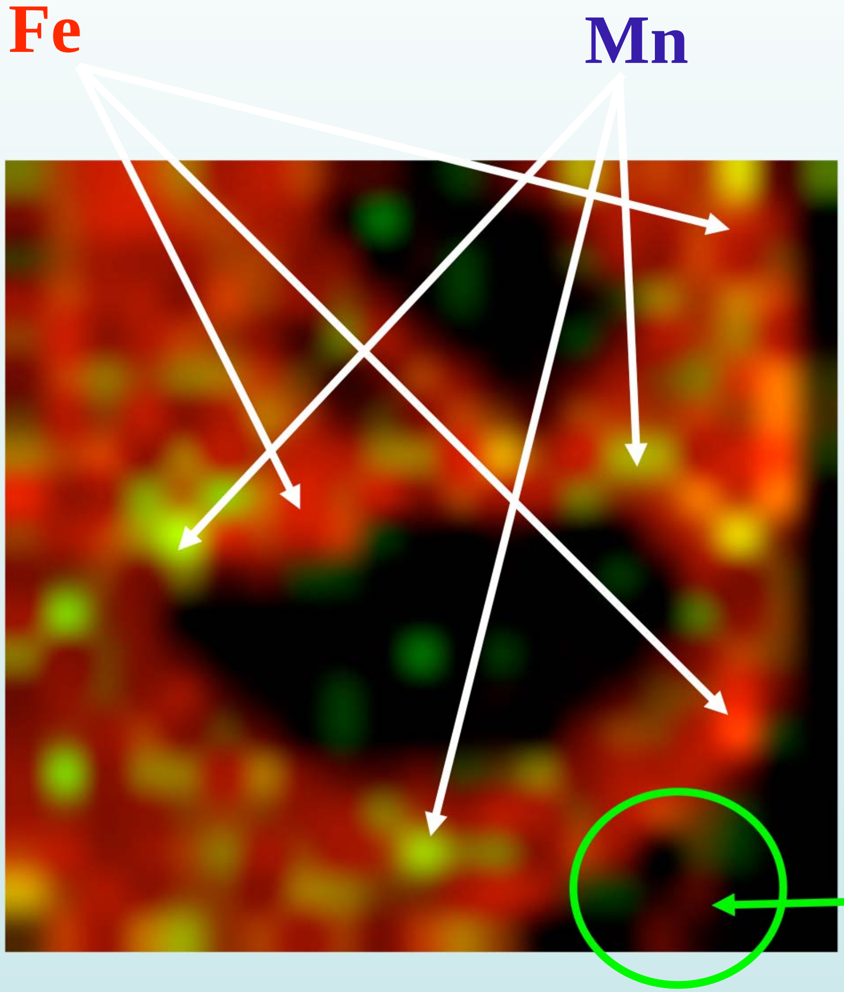

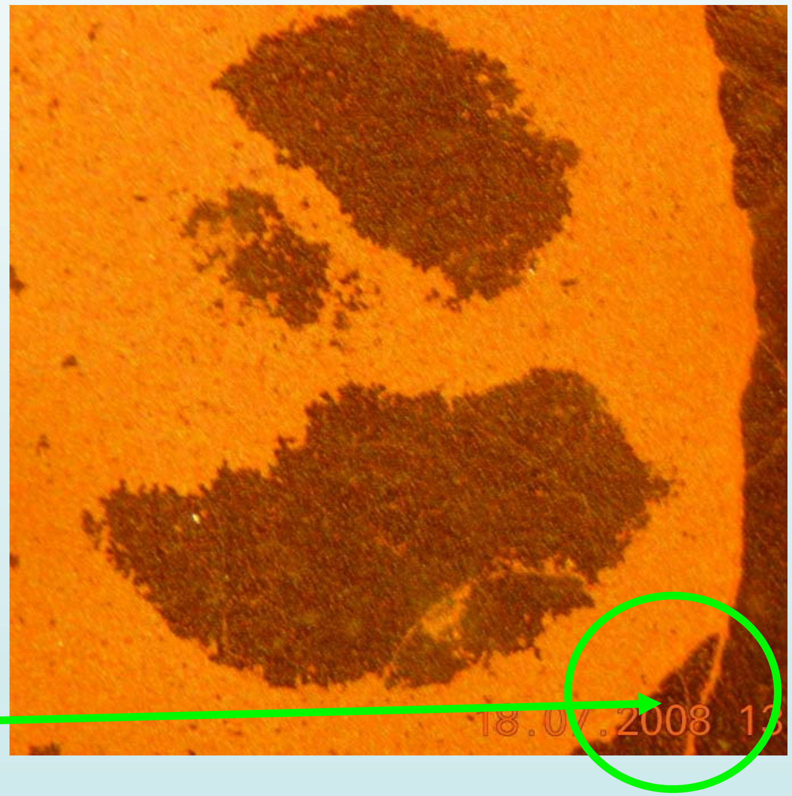

@ polyCO + Spherical CRL

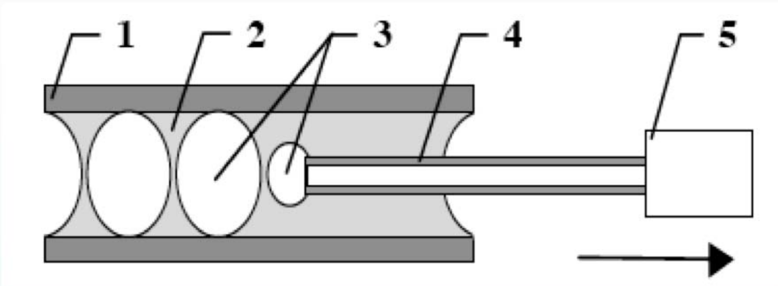

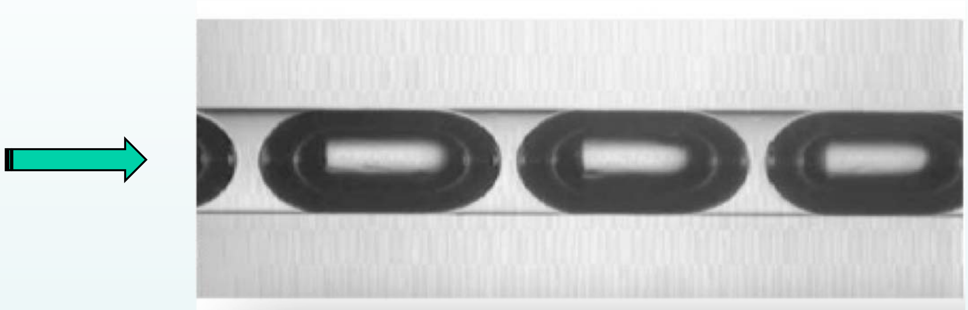

μXRF + μX-imaging = polyCO confocal + spherical (“buble”) compound refractive lens

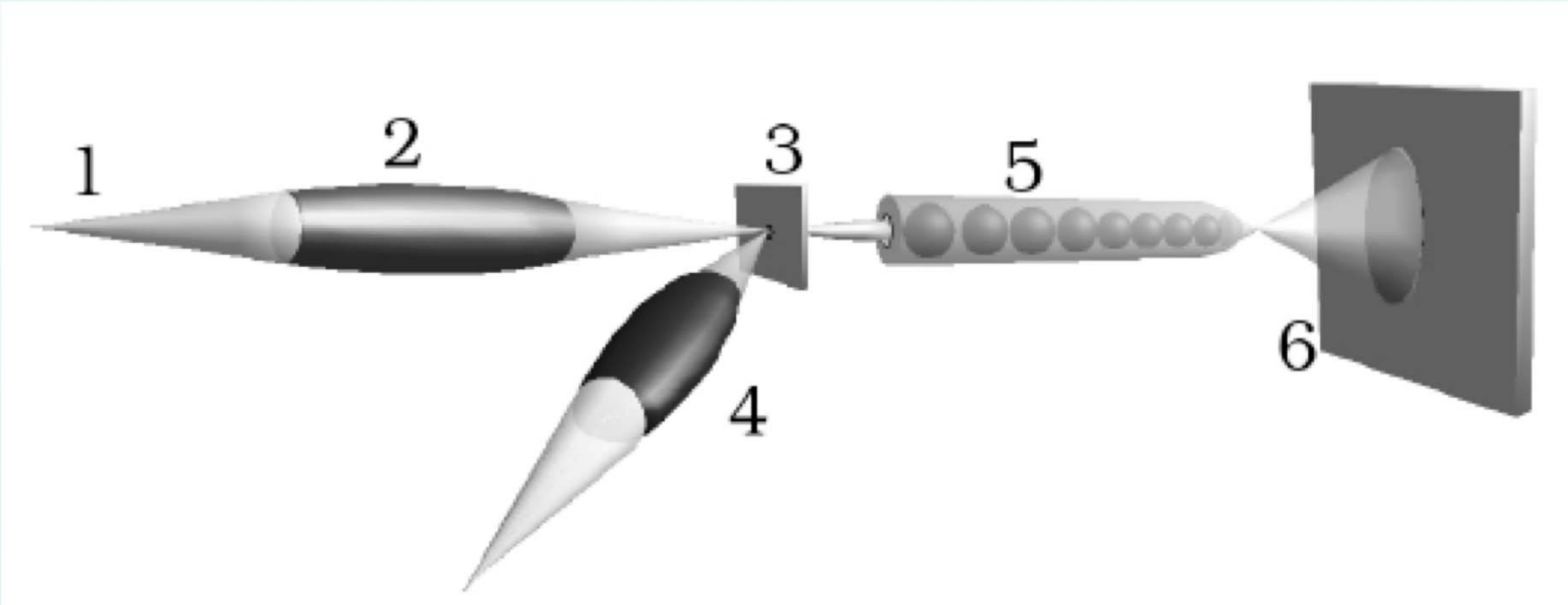

@ g-lens → graded lens

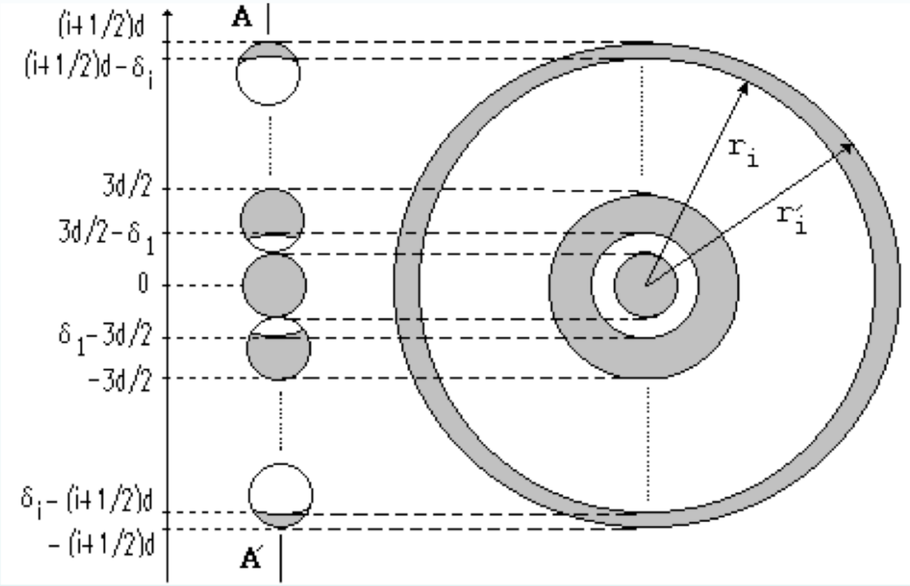

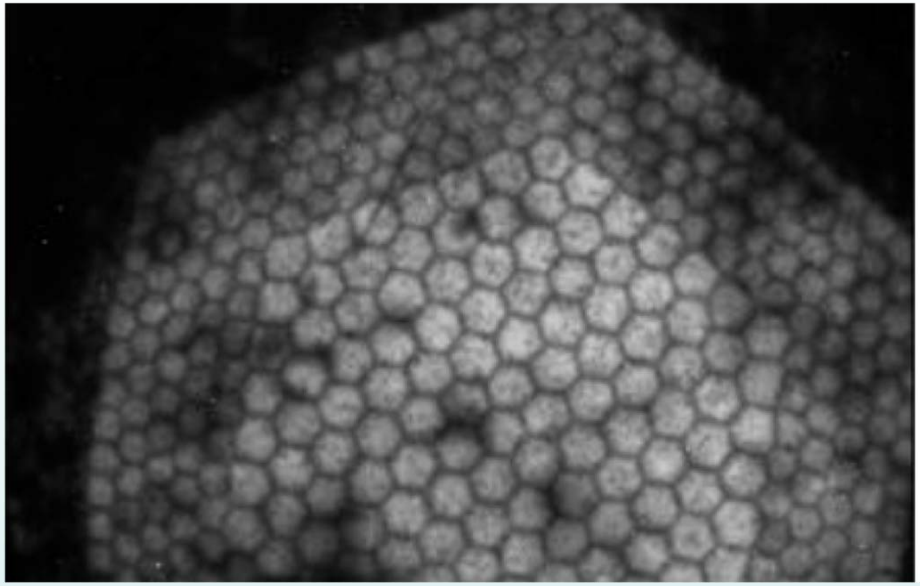

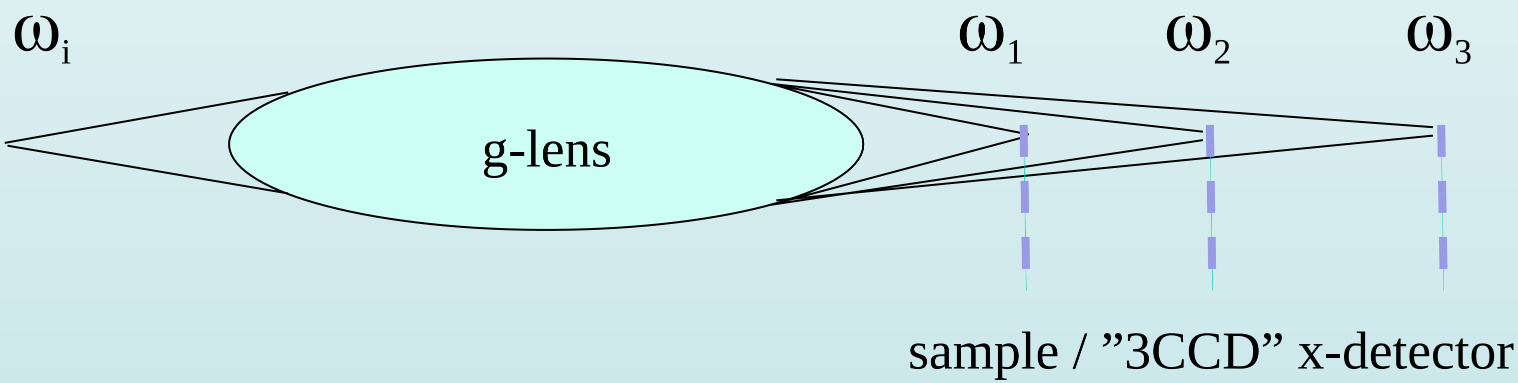

@ GEM X-Ray Spot with Polycapillary: GEMINI

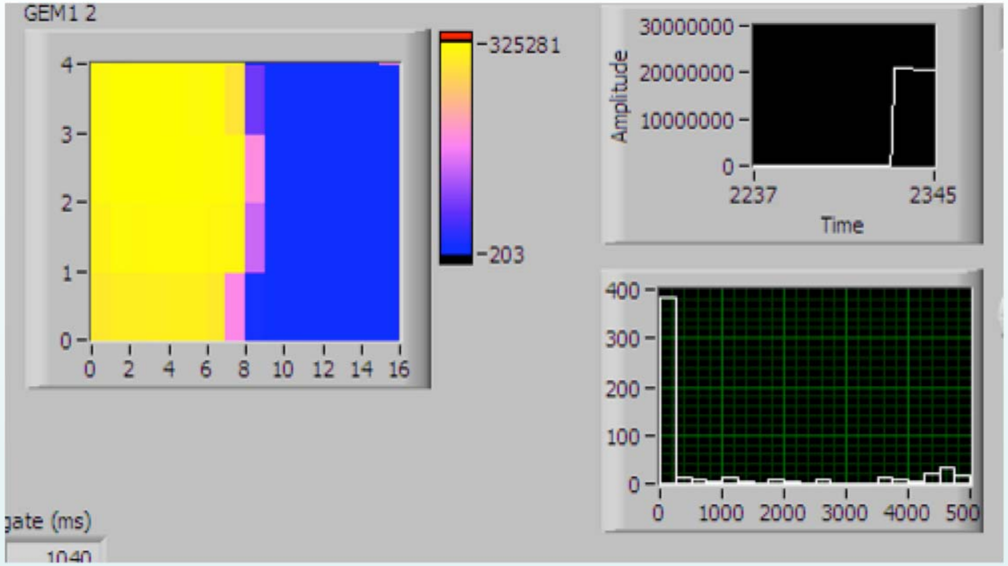

3x6 mm^2 pads

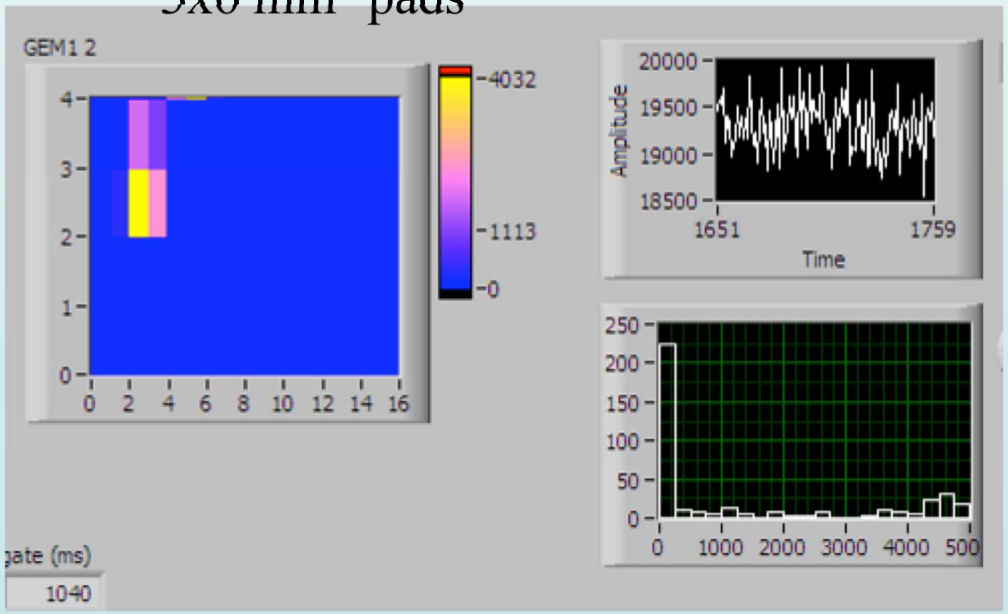

Before

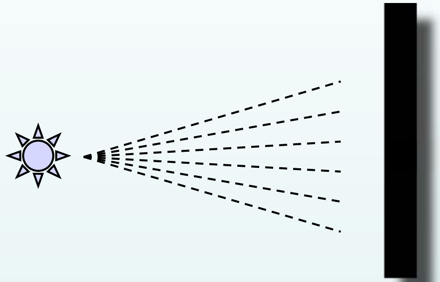

3GEM detector

First measurements with polycapillary and GEM detector

After

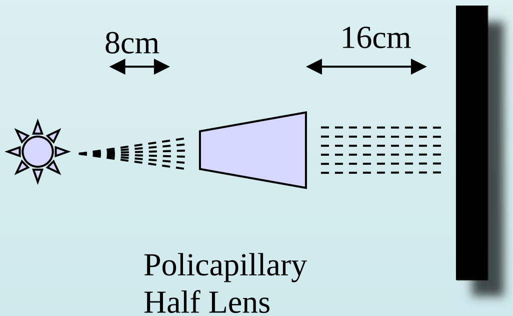

3GEM detector

@ Measurements with 3GEM

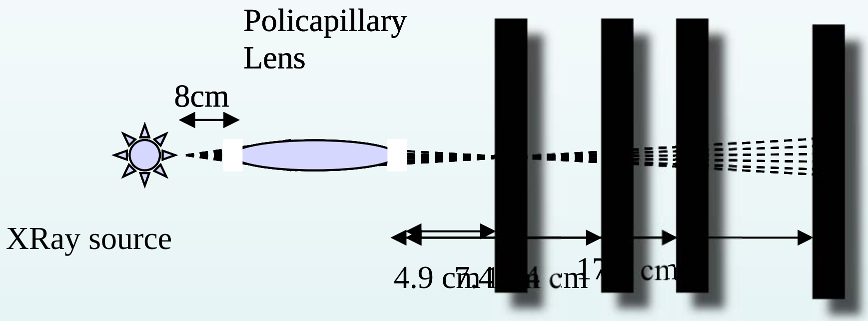

3GEM
detector

X Ray Energy 10.6 kV
Current 0.01 mA Power 0.1 Watt
3GEM Plateau @ 980 Volt (AR CO_2 CF_4)
GEM spot counting rate 380 Hz
Efficiency X Ray detection 7 %

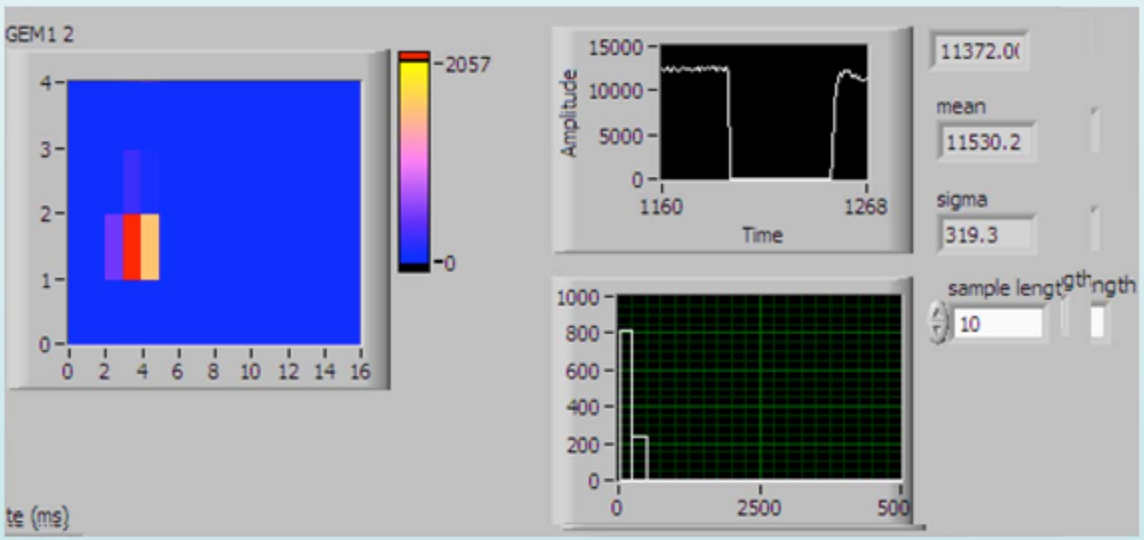

@ Linearity: GEM detector

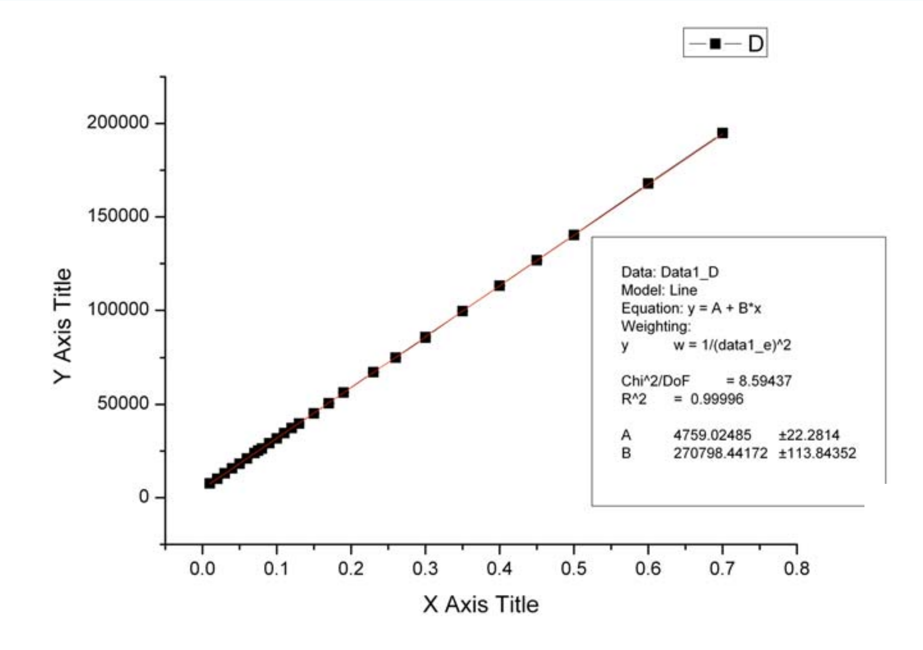

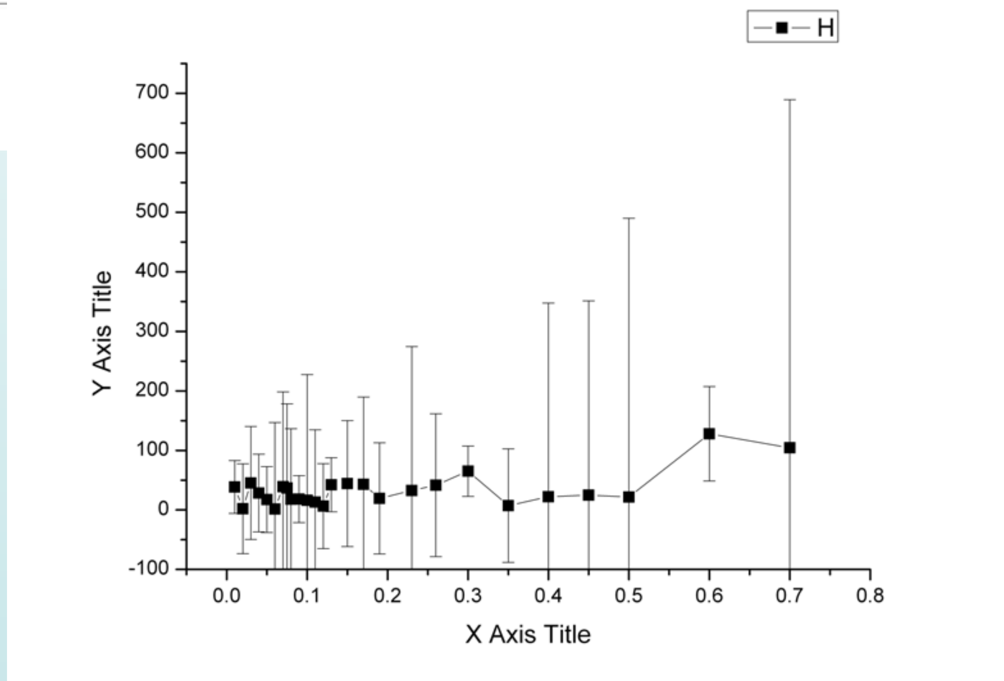

@ Down to bulk X-ray channeling

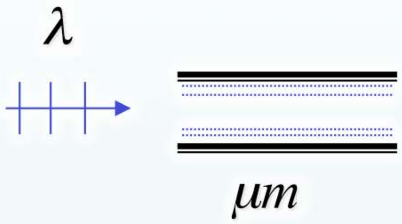

$\theta << 1 \quad (\theta_c \sim 10^{-3})$: *grazing incidence optics*

$\lambda \quad \rightarrow \quad \lambda_\perp >> \lambda$: *from nm to μm*

$d_0 \sim 1\mu m \div 10\mu m: \quad \lambda_\perp << d_0$: *surface channeling*

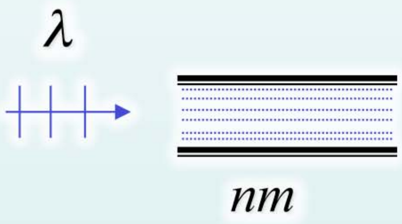

$\theta_d = \lambda/d_0 \sim \theta_c$: *diffraction angle approaches Fresnel angle*

$\lambda_\perp / d_0 \sim 1$: *bulk channeling*

* *Channeling: charged particles ⊕ crystals*
Example: e⁻ captured by the string potential (smeared atomic)

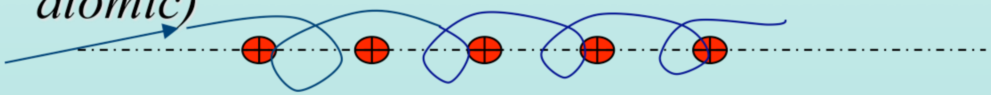

averaged potential

$\varphi << 1 \quad (\varphi < \varphi_L \sim \sqrt{U/E}$ – *Lindhard angle*)

@ Nanocapillaries

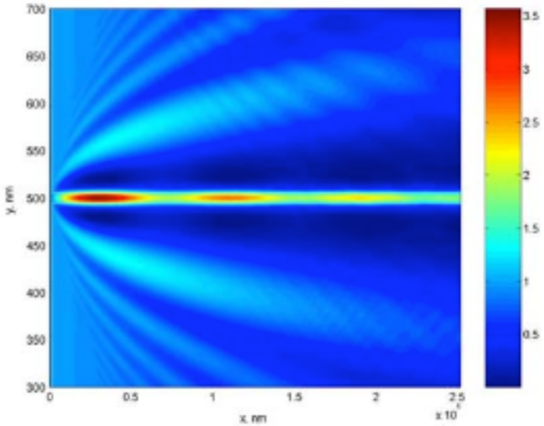

Width 10 nm

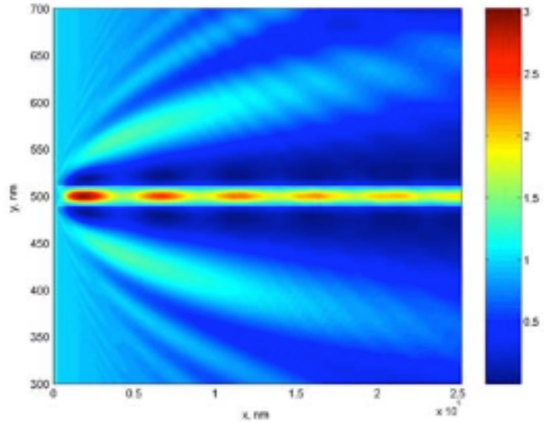

Width 20 nm

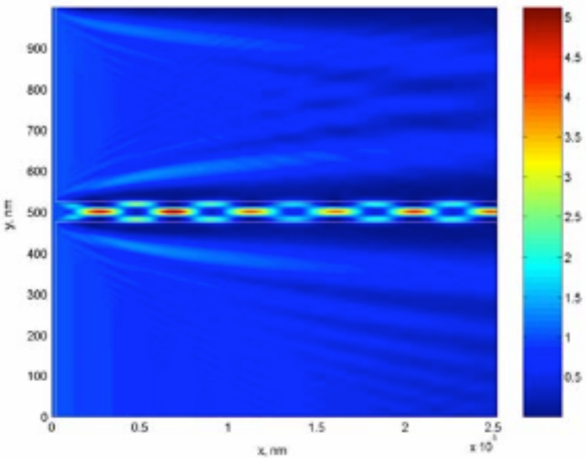

Width 50 nm

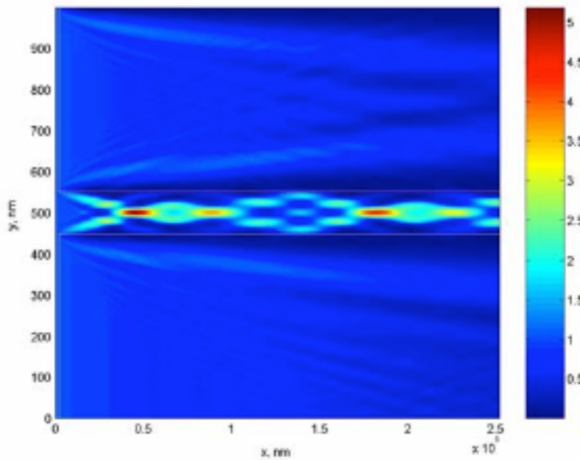

Width 100 nm

Wavelength 0.1nm, material Si, length 2*Labsorb=2.5e5 nm

$$\varsigma = \frac{2\pi\theta_c a}{\lambda} \equiv \frac{2\pi a}{\lambda_{\perp c}}$$

- number of modes

$$\lambda_{\perp c} \cong \lambda / \theta_c$$

~ 40 nm for glass

Tunneling length

$$\propto \frac{c}{\omega_p} \approx \frac{137 e^2}{\omega_p} \approx 8 \ nm$$

@ Nanotube simulations

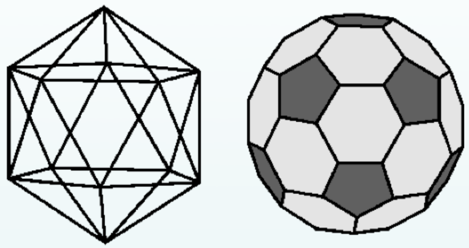

Base: *fullerene molecule C_{60}*
sphere of d ~ 0.7 nm

Nanosheet CC

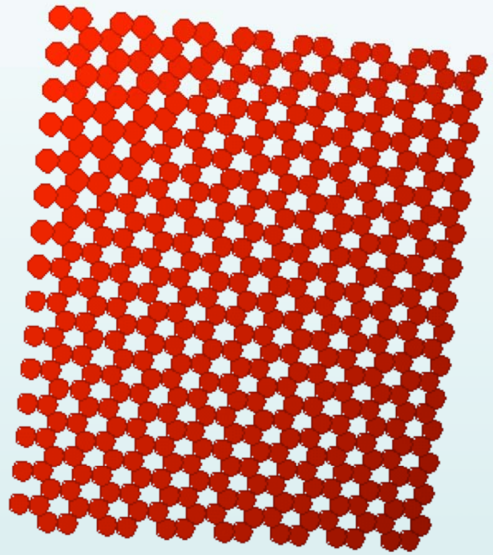

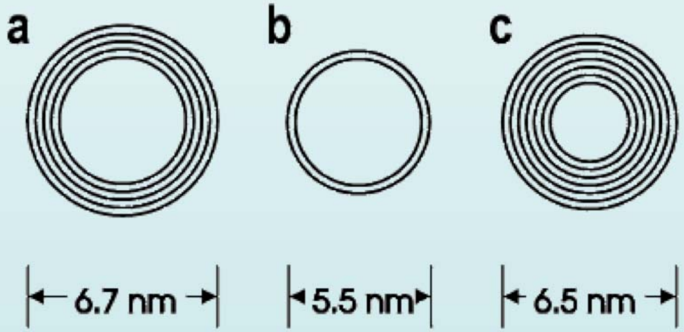

Roled graphite sheets:
nested nanotubes

@ Potentials: Doyle-Turner approximation

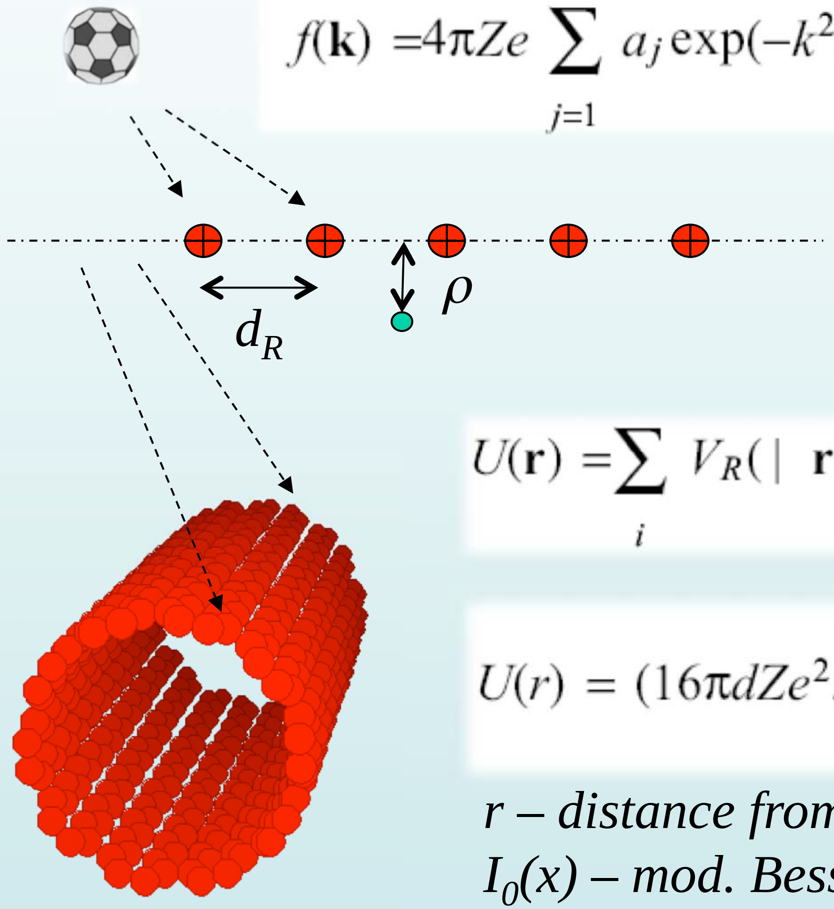

$$f(\mathbf{k}) = 4\pi Ze \sum_{j=1}^{N} a_j \exp(-k^2/4b_j^2)$$ - *form-factor for the separate fullerene*

$$V_R(\rho) = (4Ze^2/d_R) \sum_{j=1}^{N} a_j b_j^2 \exp(-b_j^2 \rho^2)$$

$$U(\mathbf{r}) = \sum_i V_R(|\ \mathbf{r} - \mathbf{r}_i\ |)$$

continuum potential
as sum of row potentials

$$U(r) = (16\pi d Z e^2/3\sqrt{3}\, l^2) \sum_{j=1}^{N} a_j b_j^2 \exp\{-b_j{}^2[r^2 + (d/2)^2]\} I_0(b_j^2 r d)$$

r – distance from the tube
$I_0(x)$ – mod. Bessel function

@ Potentials: Doyle-Turner approximation

Continuum potential in C60 fullerite: [100] and [110] after averaging of the wall potential

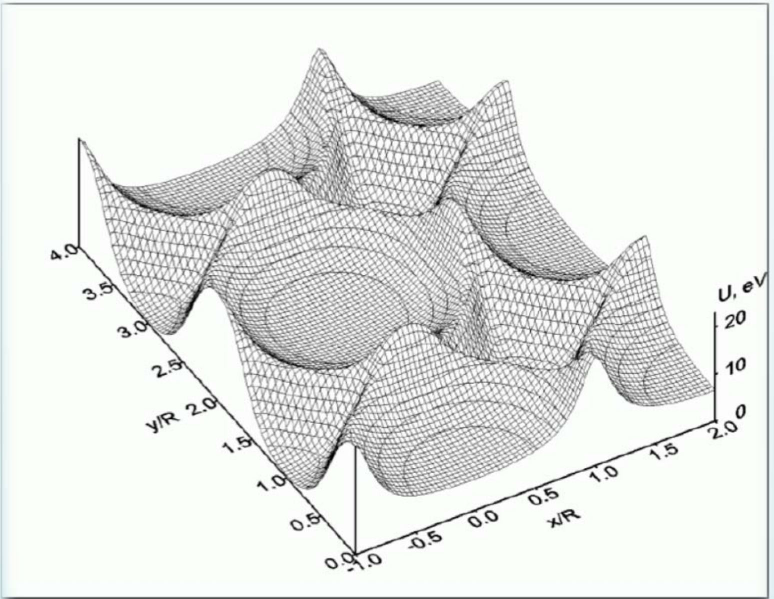

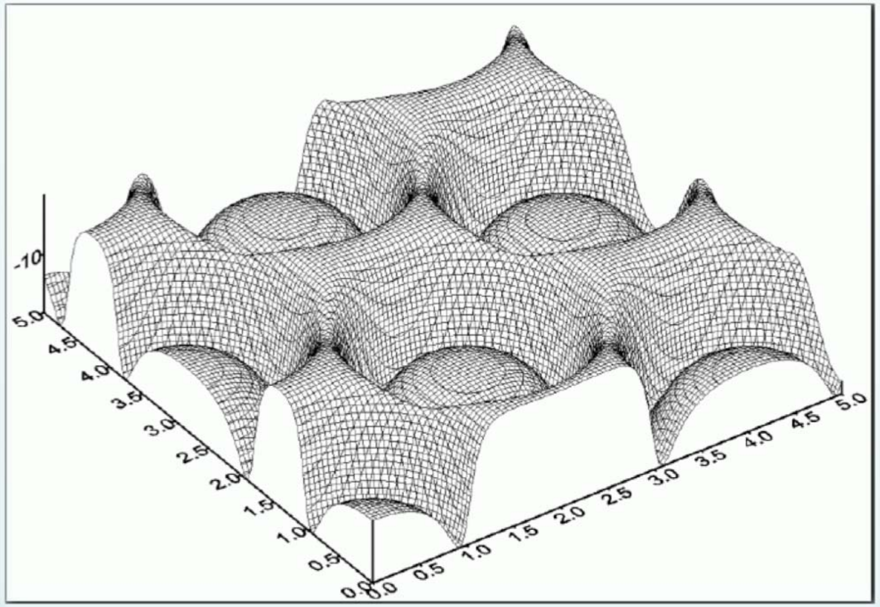

@ Potential for neutral particles: Moliere approximation

$$N_e(r) = \frac{Z}{4\pi a^2 r}\sum_{i=1}^{3}\alpha_i\beta_i^2\exp\left(-\frac{\beta_i r}{a}\right)$$

$$C: \quad Z = 6$$

$$a \approx 0.05 Z^{-1/3} - \quad screening \quad length$$

$$\overline{N}_e(r) \approx \frac{r_{curv} n_a Z}{\pi a^2}\sum_i \alpha_i \beta_i^2 \int_0^{\pi} d\theta K_0\left(\frac{\beta_i \rho}{a}\right)$$

$$\rho = \left(r^2 + r_{curv}^2 - 2 r r_{curv}\cos\theta\right)^{1/2}$$

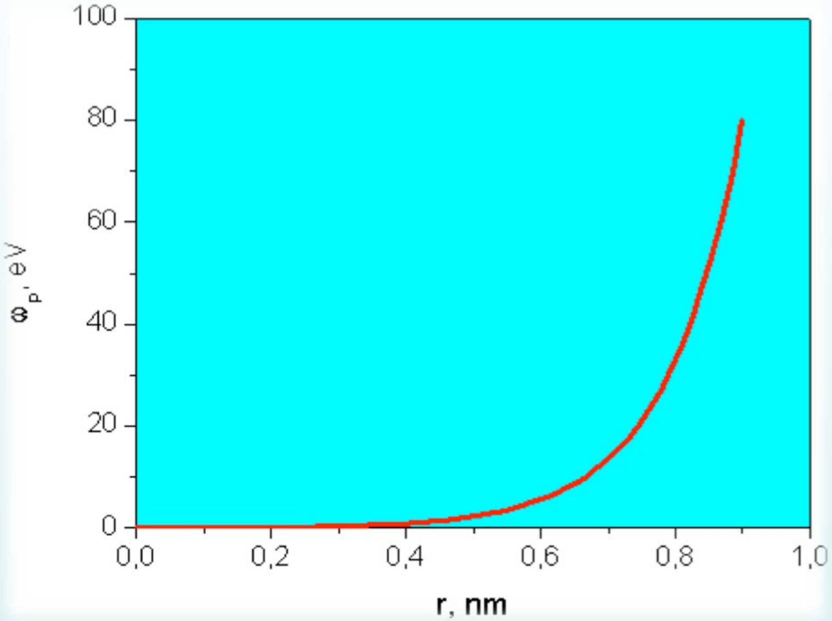

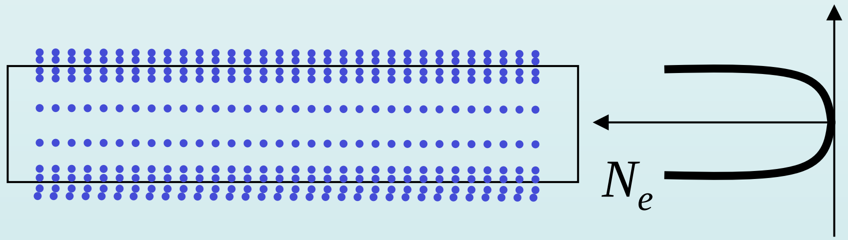

"Continuous filtration by energy"

@ Nanocapillary: *Bending efficiency*

$$n = \sqrt{1-\theta_c^{\,2}} \approx \sqrt{1-\frac{\omega_p^{\,2}}{\omega^2}}$$

$$\omega_p = \sqrt{\frac{4\pi N_e e^2}{m}} - \quad plasma \quad frequency$$

$$\omega - \quad photon \quad frequency$$

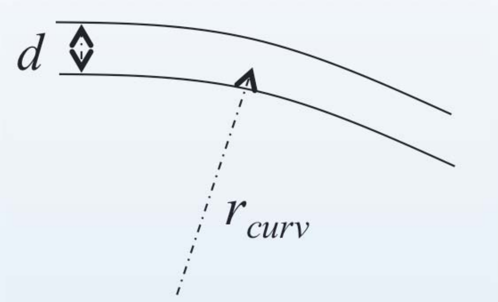

Effective bending:

$$\frac{r_{curv}\theta_c^{\,2}}{2d} \geq 1$$

μ-capillary: 10^0-30^0 through 10-20cm

n-capillary: the reduce of the dimensions by several orders with much higher efficiency of the bending

@ Bulk channeling: *tunneling & diffraction*

The even modes exists at any ratio between the channel size and layer distance

Leakage through barrier

"Tunneling"

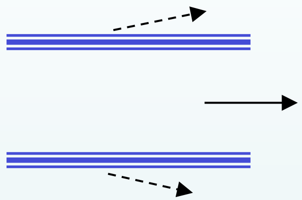

$\lambda_{\perp} \sim 100$ A

$\lambda_{\perp} > (>>)\ \Delta d$

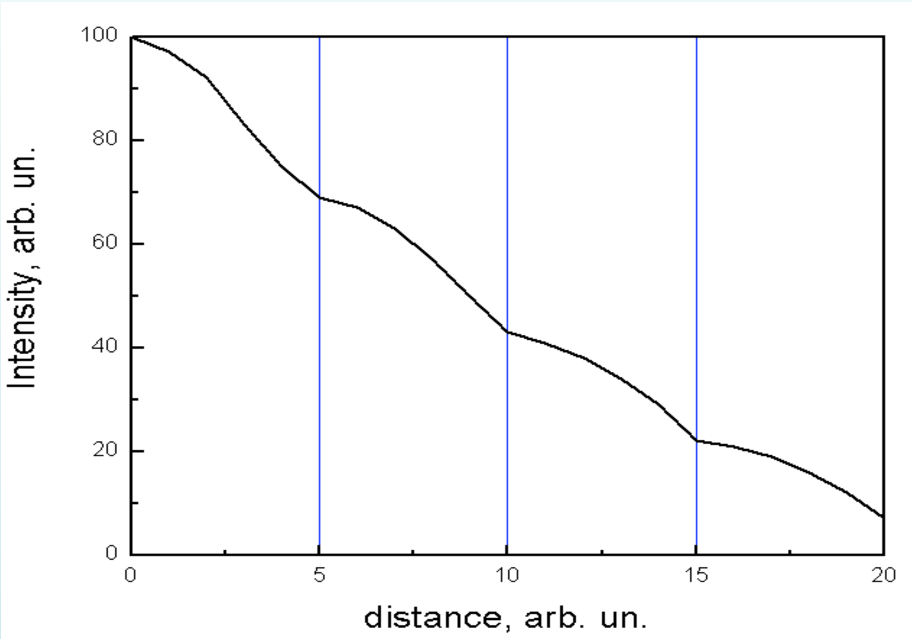

Spatial distribution of radiation through the various narrow channels

Evidence of high leakage through the nanotube wall barriers

–

The necessity of the cladding - multiwall nanotube

@ Nanotube sample – forest of nanotube bundles

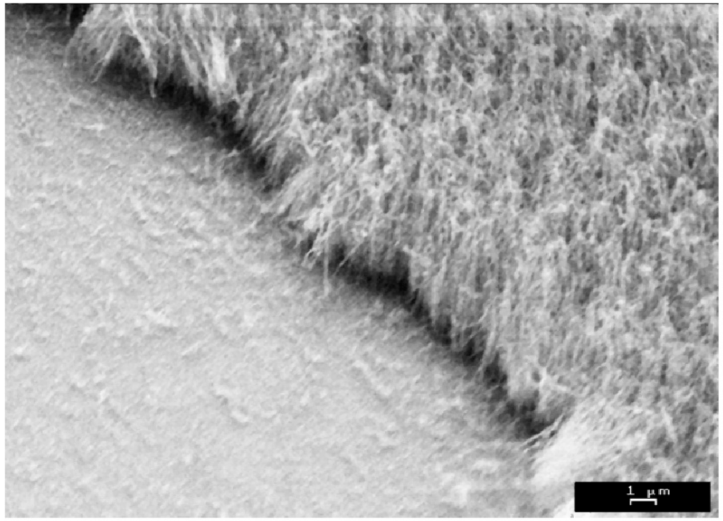

SEM image of aligned carbon nanotube bundles deposited perpendicularly to the substrate surface.
<L> ~ 10 μm.

By TEM investigations, multilayered carbon nanotubes, making film structure, have from 5 up to 25 layers, external diameter of 100÷200 Å, and diameter of an internal cavity of 50÷70 Å.

Angular distribution for nanotube forest

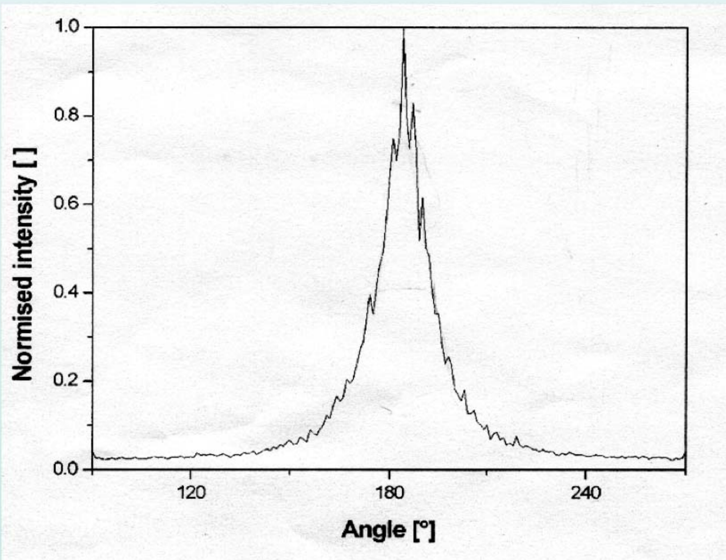

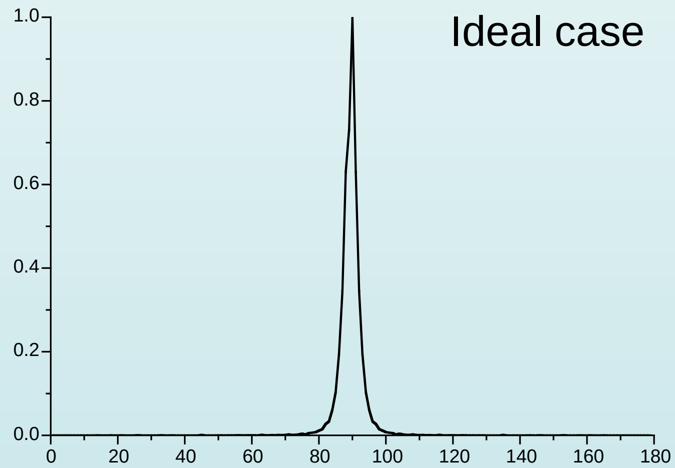

@ X-ray channeling in nanotube

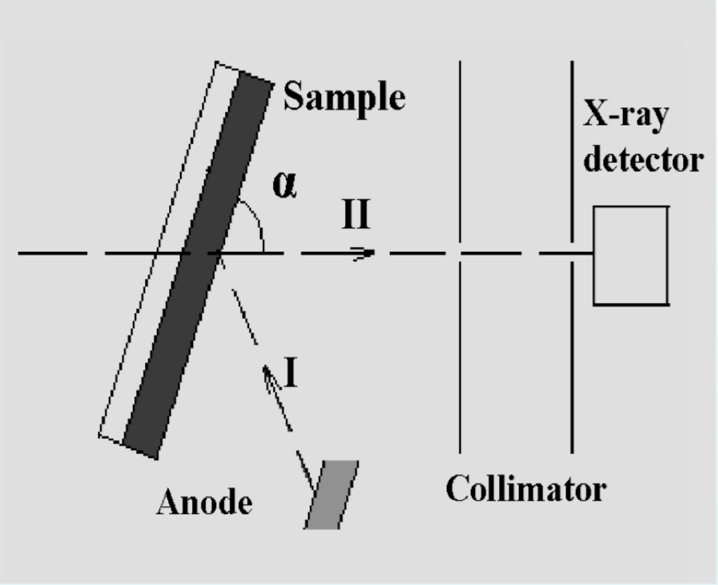

The sample of 8 mm in length and 2 mm in width was fitted to the rotatable axis provided the change of angle α between the sample surface and the optical axis of spectrometer from 60^o to 100^o. The angle β between the radiation source (anode surface of 6 mm in width) and the rotating axis was 20^o.

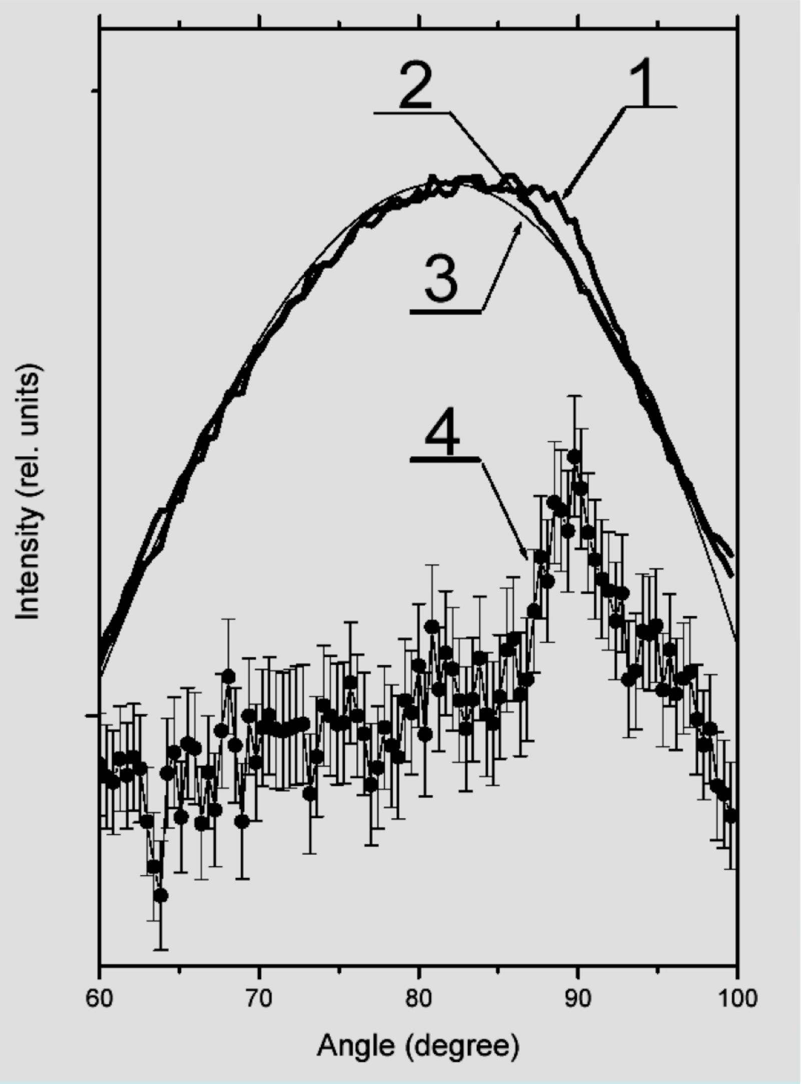

@ X-ray channeling in nanotube: estimations

Diffuse scattering +Inner cavity

$$\langle \Delta\theta \rangle_{text} + \langle \Delta\theta \rangle_{pass}$$

$$\langle \Delta\theta \rangle = \langle \Delta\theta \rangle_{diff} + \langle \Delta\theta \rangle_{chan}$$

20^0-30^0

$$\langle \Delta\theta \rangle_{chan} \sim \frac{1}{r_0 N_0} \int_{\omega_{\min}}^{\omega_{\max}} d\omega \, \frac{N(\omega)}{\omega} \int_0^{r_0} dx \, \omega_0(x)$$

$\langle \Delta\theta \rangle_{chan} \lesssim \omega_{0\,\max} r_0/10 \approx 6^0 \div 10^0$ at the given values of $\omega_{0\,\max} \simeq 100 \div 150$ eV

@ Features of C Kα propagation in nanotubes

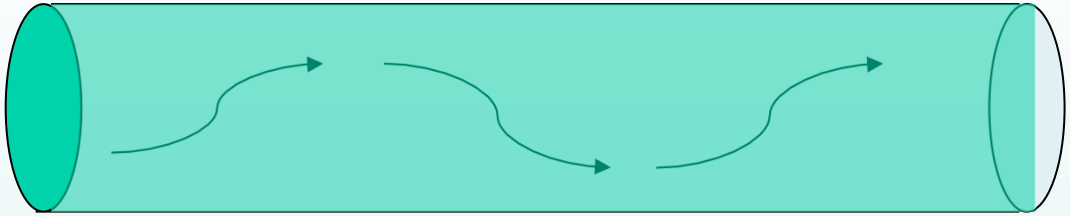

$n = 1 - \delta = \cos\varphi_0/\cos\varphi$

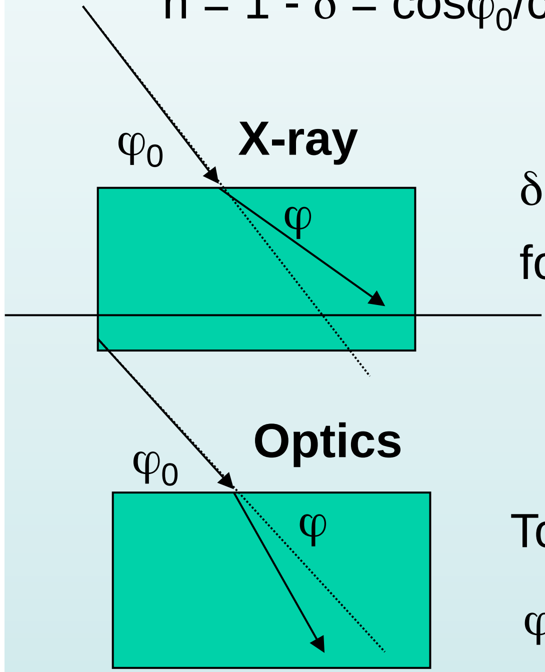

$\delta \sim 10^{-6}$ $\lambda \sim 0.1$ nm for C media

for $\omega >> \omega_l$ $\delta = r_0 N \lambda^2/2\pi$

Total internal reflection:

$\varphi_0 \sim \sqrt{2\delta} \sim 2.5°$ for $\delta \sim 10^{-3}$

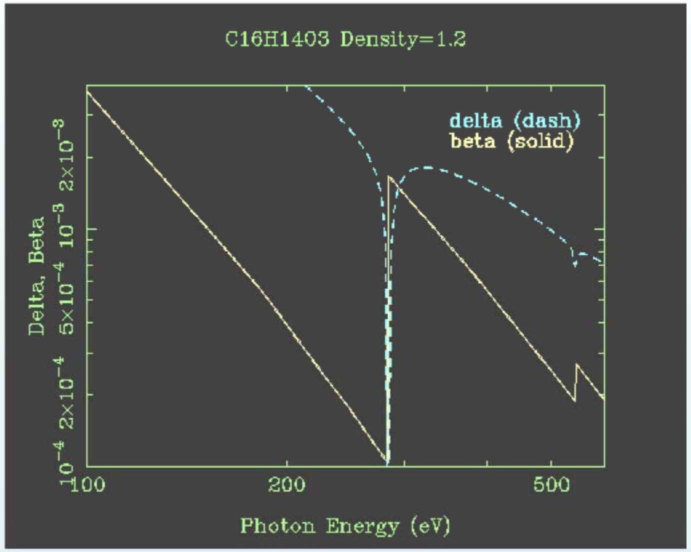

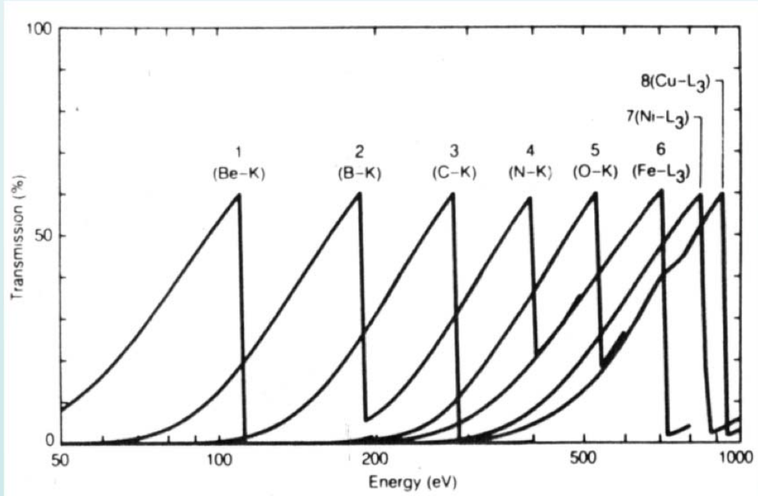

Fig. 2-7. Transmission bands of selected filters (see table) between 50 eV and 1 keV.

@ X-ray nanotube channeling: *possible applications*

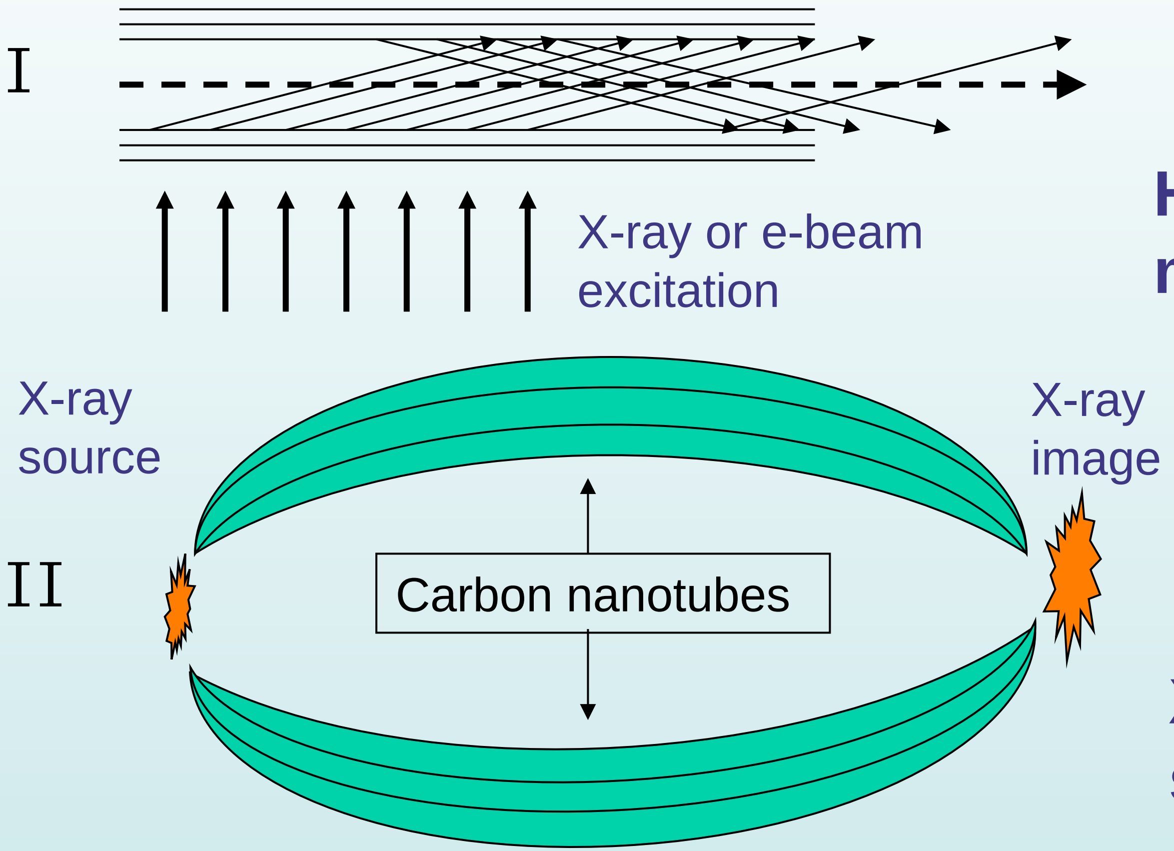

High- brilliance X-ray micro- sources

X-ray nano-focusing system

@ Capillary Optics as Instrument

@ focusing efficiency:

condensing radiation in a spot of submicron & nanometer diameter with flux gain of 10^3-10^5

- x-ray spectroscopy (XRF analysis - min. detect. limit up to 10^{-15} g)
- x-ray microscopy (source image study - nm scale: μ-CHANDRA)
- μ-diffraction (XRD analysis - analysis of micro-materials: “table synchrotron”)

@ bending efficiency:

deflection through the angle up to 30^0 over the distance 10-15 cm

- special angle-tuning bender (space problem for new experiments)

@ new technological ideas:

combination of various types of optics

@ X-ray waveguiding for *basic research*

surface x-ray and neutron channeling

@ *bound states of x-ray propagation through capillary channels*

- **quantum effects in curved space (*simple model of gravity*)**
- **coherent/incoherent x-ray & n scattering study (*whispering gallery for x-rays*)**
- **phase distortion study (“*hidden coherence*”)**

bulk channeling of neutral particles & modal propagation

@ *nanotubes as nanocapillaries (?):*

- **new instrument to study bulk parameters of nanotubes (*bulk potentials etc.*)**
- **novel x-ray & n optical devices (*nanofocusing, nanocollimation etc.*)**

@ *nanochannels as nanocapillaries (!):*

- **X-ray & n “hollow fibers” – inverse to optical waveguide**

…

Thanks to

the international collaborations

in

Channeling and X-ray Optics

Projects,

particularly:

D. Hampai, G. Cappuccio, G. Cibin, F. Murtas, I. Bukreeva, A. Popov

...